Final report

Rapiscan RTT-110 system upgrade accuracy validation

Project code: V.TEC.1722

Prepared by: H.B. Calnan, M.T. Corlett, S.E. Connaughton, G.E. Gardner
Murdoch University

Date published: 14/05/2021

PUBLISHED BY
Meat & Livestock Australia Limited
PO Box 1961
NORTH SYDNEY NSW 2059

Meat & Livestock Australia acknowledges the matching funds provided by the Australian Government to support the research and development detailed in this publication.

Abstract

The Rapiscan RTT-110 X-ray system has potential to produce rapid 3-D scans of beef or lamb to predict carcass composition and inform automated boning at abattoir line speed. To investigate this 15 beef primals (rib sets and short loins) and 30 lamb carcasses selected to represent a wide range in weight and fatness were scanned by the Rapiscan RTT-110 and a medical CT system – the current gold standard measure of carcase composition. To assess image resolution and dimension estimation an XTE-CT test piece was also scanned. Image analysis showed the RTT-110 system can clearly identify bone tissue in beef primals and lamb carcases. Initial analysis indicated that the RTT-110 could estimate medical CT fat % with good precision and lean % with moderate precision in beef short loins and lamb carcases. Alternatively, with estimation of CT fat% and lean% in beef rib-sets was poor. Upon closer inspection, the apparent ability of the RTT-110 to identify fat in beef short loins and lamb carcases appears to be principally a result of tissue thresholding in RTT-110 images incorrectly identifying the outermost tissues as fat tissue, thus Hu values were merely reflecting tissue depth. Hence in beef rib sets, where the fat tissue was predominantly located internally between muscle groups, the RTT-110 could not predict CT fat% or lean %. Alternatively, the image resolution and capacity to measure in a highly repeatable fashion, as demonstrated through scans of the XTE-CT test piece, demonstrates the capacity of this device to provide accurate 3-dimensional imagery suitable for automation. Therefore, while the Rapiscan RTT-110 is suitable for directing automated cutting based on bone landmarks, further calibration work is needed to improve RTT-110 differentiation of fat and lean tissue via tissue thresholding in lamb and beef products.

Executive summary

This report assessed the ability of Rapiscan RTT-110 CT scanner to differentiate tissue types, and determine fat%, lean% and bone% in lamb carcases, beef rib-sets, and beef shortloins. Evaluation of image resolution and dimension estimation was also undertaken using the XTE-CT test piece. Key outcomes were as follows:

1. The Rapiscan RTT-110 demonstrated excellent capacity to differentiate bone from soft tissues in lamb and beef. This was evident through visual assessment of anatomical structures and through the high precision estimate of bone%.
2. The Rapiscan RTT-110 demonstrated limited capacity to differentiate fat from lean tissue. This was evident through visual assessment of anatomical structures and through the high precision estimate of bone%. Inspection of RTT-110 images indicated that fat and lean tissue, and seams between muscle depots, could be visually differentiated. However, these tissues could not be well differentiated via pixel thresholding methods. Therefore, the ability of the RTT-110 images to predict medical CT composition in lamb and beef was highly variable. Pixel thresholding of RTT-110 images was related to tissue depth in beef and lamb scans, with soft tissue pixels located in the surface regions allocated lower pixel values and thereby identified as fat.
3. Image resolution and ability to measure in a scaled and highly repeatable fashion, as demonstrated through scans of the XTE-CT test piece, demonstrates the capacity of this device to provide imagery suitable for automation.
4. Further calibration work is therefore needed on RTT-110 images to ensure pixel values across a primal or carcase image are consistently associated with tissue type density, allowing consistent allocation of fat and lean tissue throughout the cross-sectional scan and thereby more precise estimates of beef and lamb carcass composition and identification of seams separating soft-tissue depots.

Table of contents

1. Background

The development of novel X-ray technologies provides many opportunities to improve the efficiency of red meat production and processing in Australia. Medical computed tomography (CT) is now considered the gold standard imaging method for assessing and quantifying different tissue types in lamb and beef carcasses; providing a complete 3-D virtual dissection of carcasses or carcass components. While the slow speed and expense of medical CT scanning prevents its commercial use, this device is used as the gold standard in the training and testing of novel technologies aiming to predict the composition of lamb or beef.

In addition to the potential to improve measurement of carcass composition or lean meat yield; X-ray technologies also offer the opportunity to improve the automated deboning of lamb and beef. While currently 2-D X-ray images are adequate to provide the precise skeletal coordinates to direct the automated cutting of lamb carcasses, in the beef industry commercial cutting lines predominantly involve the identification of seams between muscles and fat depots and therefore 3-D imaging of beef carcasses or primals is needed to advance automation.

Rapiscan X-ray systems may have the capacity to produce rapid 3-D scans of beef and lamb to predict carcass composition and inform automated boning at line speed. Rapiscan have manufactured imaging components and software to adapt the RTT-110 airline inspection CT scanner for carcass assessment. However, the ability of this system to differentiate tissue types and thereby determine bone landmarks, muscle seams and lean meat yield in beef primals and lamb carcasses when compared to medical CT needs to be determined.

2. Objectives

The objective of this report was to assess the ability of Rapiscan RTT-110 images to differentiate fat, lean and bone tissue and thereby to determine bone landmarks, muscle seams and CT lean meat yield % in beef rib sets, short loins, and lamb carcasses.

3. Methodology

3.1 Beef primal selection

Fifteen carcasses were selected from Teys Wagga Wagga abattoir in New South Wales to achieve a wide phenotypic range in carcass weight (kg) and fatness (mm) for this experiment. A bone-in beef rib set (AUSMEAT item 2220) and bone-in short loin (AUSMEAT item 1552, without the tenderloin) were selected from each carcass for the scanning experiment. Primals were vacuum packaged, weighed and labelled before being transported chilled to Melbourne Jet Base for Rapiscan RTT-110 scanning. The weight, P8 fat depth and primal weights of the selected carcasses are shown in Table 1.

Table 1. The hot standard carcass weight, P8 fat depth, rib set and short loin primal weight for the 15 beef carcasses scanned in this experiment.

Carcass number	Carcass weight (kg)	P8 fat depth (mm)	Rib set weight (kg)	Short loin weight (kg)
1	343.2	21	10.8	9.7
2	374.6	20	12.3	9.6
3	368.6	20	12.2	10.8
4	388.2	23	12.9	11.4
5	394.6	13	11.2	10.9
6	332.2	13	10.5	9.4
7	320.6	7	10.7	8.9
8	364.2	8	12.0	10.1
9	365.8	10	11.9	9.7
10	196.8	3	7.1	5.0
11	193.2	3	6.7	5.2
12	205.2	12	6.7	5.6
13	219	10	7.9	6.6
14	301.4	12	9.2	7.9
15	366.2	26	13.1	9.6

3.2 Beef primal scanning

At approximately 10 days aging, the 15 rib sets and 15 short loins were scanned by the Rapiscan RTT-110 system at a speed of 25mm/sec over a two-day period. An XTE-CT calibration test piece was scanned at the same speed before and after the beef primal scans. The RTT-110 images were provided to Murdoch University in DICOM format for analysis.

Figure 1. Rapiscan RTT-110 scanning of a beef rib set.

On arrival via chilled-transport to Murdoch University, the primals were re-weighed. Some vacuum packaging had been pierced by sharp bone edges during transport and thus leaked small amounts of fluid or exudate. Following standard calibration of the CT scanner (a Siemens Somatom Scope 16 slice CT scanner) using air and water, all rib sets and short loins were CT scanned at settings of 110 mA, 135 KV and at 1mm slice thickness. The CT scanner had a field of view of 480mm, a pitch of 1, rotation time of 0.8 seconds and was set to an Abdomen soft tissue algorithm. The XTE-CT calibration test piece was also scanned using the same settings as the beef section scans.

Figure 2. Medical CT scanning of a beef short loin and rib set.

3.3 Lamb carcass selection

Thirty lamb carcasses were selected from Frewstal abattoir in Victoria to achieve a wide phenotypic range in carcass weight (kg) and fatness (mm). Carcasses were split into three sections; the fore section, saddle and hind. The fore section was separated from the saddle by a cut between the fourth and fifth ribs, and the hind section was separated from the saddle by a cut through the mid-length of the sixth lumbar vertebrae. Carcass sections were weighed, labelled, strung together to hang on a hook and wrapped in muslin fabric for transport chilled to Melbourne Jet Base for Rapiscan RTT-110 scanning. The hot standard carcass weight and GR tissue depth of the selected carcasses are shown in Fig. 3.

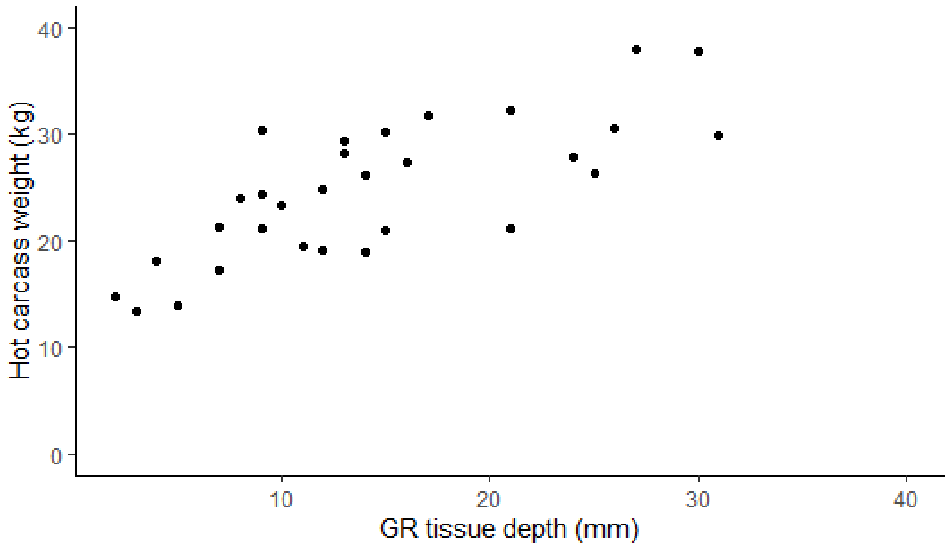

Figure 3. The hot standard carcass weight and GR tissue depth of the 30 lamb carcasses.

3.4 Lamb carcase scanning

At between 48 – 72 hours post-mortem, the fore, saddle and hind sections were scanned by the Rapiscan RTT-110 system at a speed of 25mm/sec over a two-day period. The XTE-CT calibration test piece was scanned at the same speed before and after the lamb section scans. RTT-110 images were provided to Murdoch University in DICOM format for analysis.

Carcass sections were re-labelled, strung together and re-wrapped in muslin fabric for chilled transport to Murdoch University for medical-CT scanning. The lamb sections were weighed and the saddle was cut into two components prior to CT scanning. The lamb fore sections ranged from 7.7kg to 12.4kg, averaging 8.35kg (±2.08); the saddle section ranged from 3.6kg to 13.1kg, averaging 7.52kg (±2.38), and the hind section ranged from 4.9kg to 12.5kg with a mean weight of 8.54kg (±1.99). The saddle section was cut at the $12^{th}/13^{th}$ rib so that the short loin could be positioned within the rib set for medical CT scanning.

Following standard calibration of the medical CT scanner (a Siemens Somatom Scope 16 slice CT scanner) using air and water, an entire lamb carcass was CT scanned at settings of 110 mA, 120 KV and at 5mm slice thickness. The CT scanner had a field of view of 480mm, a pitch of 1, rotation time of 0.8 seconds and was set to an Abdomen soft tissue algorithm. The XTE-CT calibration test piece was also scanned using the same settings as the lamb section scans.

Figure 4. Medical CT scanning of a lamb fore section, saddle and hind section.

3.5 Image analysis

Rapiscan and medical CT images of the beef primals and lamb carcasses were analysed in DICOM format using ImageJ software. Medical CT images were analysed using established protocols for the differentiation of carcass lean, fat and bone tissue %. Pixels lower than -500 were determined to be air and deleted from the image sets. The pixel Hounsfield unit thresholds used to associate pixels with fat, muscle and bone were −235 to 2.3 for fat, 2.4 to 164.3 for lean and 164.3 or greater for bone. Cavalieri's method (Gundersen et al., 1988, Gundersen and Jensen, 1987) was used to estimate volume according to the calculation:

$$\text{Volume}_{Cav} = \frac{1}{4}\, d\ \Sigma \text{areag} - t\ \text{areamax}\ g\ \frac{1}{4}\ 1$$

where m is the number of CT scans taken; d is the distance between cross-sectional CT scans (5mm); t is the thickness of each slice (g) (in this example 10 mm), and area max is the maximum area of any of the m scans.

The average Hounsfield units of the pixels of each tissue was then determined and converted into density (kg/L) using a linear transformation (Mull, 1984), and combined with the volume of each tissue to determine the weight of fat, lean and bone. These weights were then expressed as a percentage of the weight of each beef primal or lamb carcass at the time of scanning (CT fat, lean and bone %).

Rapiscan RTT-110 images were qualitatively assessed using Image J software for their ability to differentiate tissue types; to differentiate bone 3-D structural geometry, and to differentiate the seams between muscles in the beef primals and lamb sections, with the medical CT images providing a higher resolution point of comparison for tissue differentiation.

3.5.1 Beef primals

Pixel value thresholds to differentiate primal tissue for fat, lean and bone in Rapiscan images were initially determined by this qualitative assessment of images. Beef pixel values lower than 300 in RTT-110 images were determined to be air and deleted. Bone and lean tissue differentiation was estimated to be optimal at a pixel value of 1020, though varied between 1000 to 1040 in different images. Differentiation between fat and lean tissue was less clear and ranged between 740 and 840 depending on the primal type (rib set or short loins), between different primals, and even between image slices within a primal. All RTT-110 beef primal scans were therefore analysed using fat:lean thresholds of 740, 760, 780, 800, 820 and 840, and lean:bone thresholds of 1000, 1010, 1020, 1030 and 1040. After differentiating tissues in the beef primals according to these different thresholds, Cavalieri's method was used to estimate each tissue’s volume (Gundersen et al., 1988, Gundersen and Jensen, 1987) and the medical CT linear density transformation (Mull, 1984) was used to determine the weight of each tissue and calculate the percentage of each tissue type in the primal (Rapiscan fat, lean and bone %).

3.5.2 Lamb carcases

RTT-110 images of lamb sections were assessed visually to determine the optimal thresholds for differentiating bone, lean and fat tissues. The formatting of the RTT-10 lamb images made analysing the images using multiple thresholds impractical, therefore the thresholds used to analyse these images were based on this qualitative assessment alone. The RTT-110 lamb scans were therefore analysed using pixel Hounsfield unit thresholds of -250 to -50 for fat, -50 to 125 for lean and 125 or greater for bone. As in beef, after differentiating tissues in the lamb sections Cavalieri's method was used to estimate each tissue’s volume (Gundersen et al., 1988, Gundersen and Jensen, 1987) and the medical CT linear density transformation (Mull, 1984) was used to determine the weight of each tissue and calculate the percentage of each tissue type in the lamb sections (Rapiscan fat, lean and bone %).

3.5.3 XTE-CT calibration test piece

The XTE-CT test piece (Figure 1) was scanned a total of 5 times through the RTT-110 and 5 times through the medical CT-scanner.

Figure 1. XTE-CT test piece.

A number of quantitative tests were undertaken to assess the comparative image quality of these two devices. In all cases the performance of each of these tests was assessed across each of the 5 repeat scans, enabling quantification of repeatability of these performance indicators.

Simple image dimensions

In this case we assessed the scanner capacity to accurately and repeatably reflect size and thickness. For size, the diameter of a uniform 200mm section of the XTE-CT test-piece which was used for determining resolution was measured (see Figure 2). For thickness, a 40mm plastic section was detected through a series of cross-sectional scans (see Figure 3).

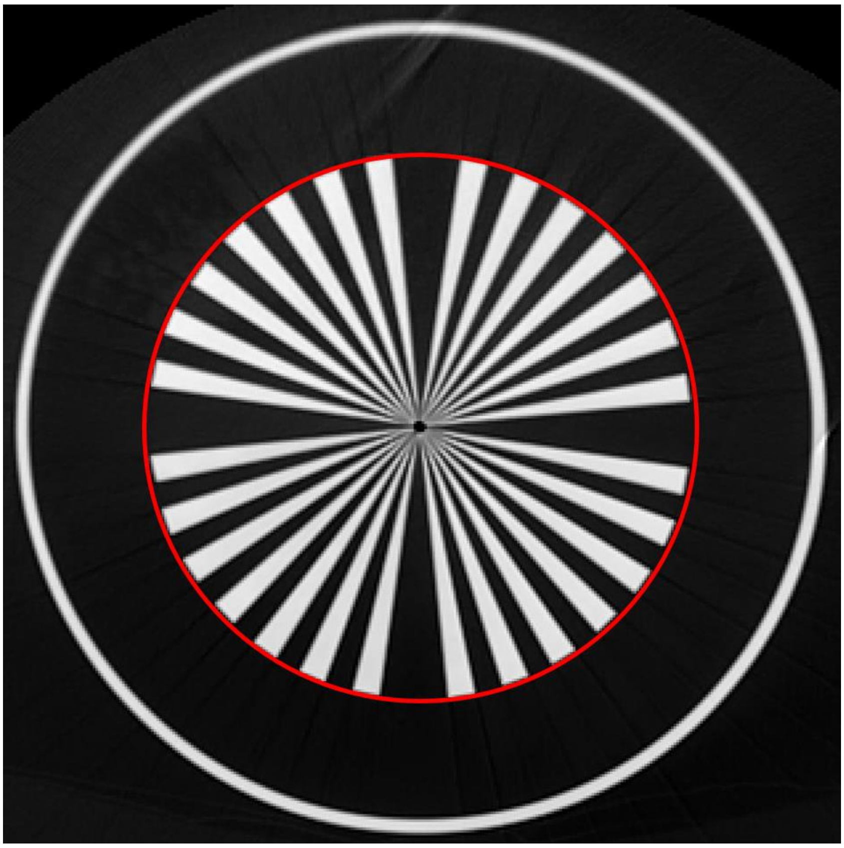

Figure 2. A simple dimension measurement was taken using the diameter of the region encompassed by the red circle shown within the figure. Within the XTE-CT test piece the diameter of this reference material was a uniform 200mm.

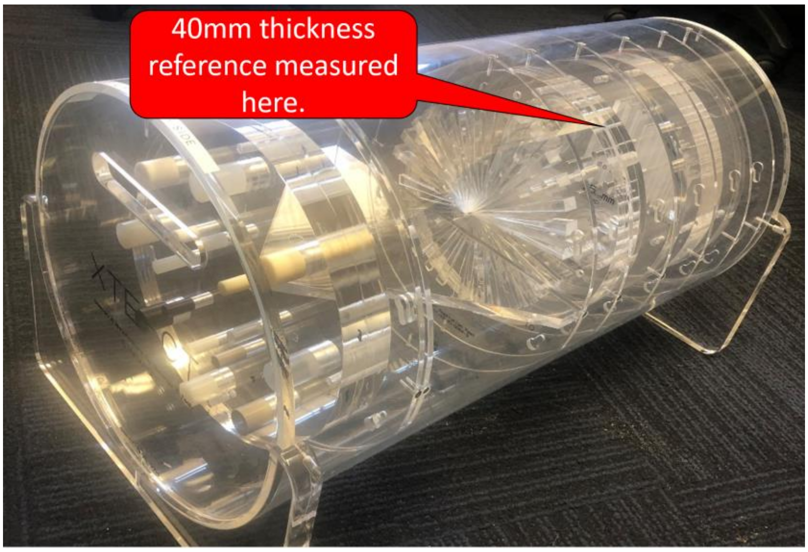

Figure 3. A simple thickness measurement was taken within the XTE-CT test piece using the section shown which was designed to be a uniform 40mm thickness.

Spatial resolution test

The spatial resolution test uses a "crows-foot" design in which tapered Perspex elements are a maximum of 10mm apart at their outer edge, tapering to a point at the centre of a circle where they meet (see Figure 4a). The test is evaluated by determining the point at which the individual elements for each thickness can no longer be resolved, corresponding to the resolution limit for the system (see Figure 4b). In this case the resolution of the system can be calculated as:

Resolution limit (mm) = 10[L1/(L1+L2)]*

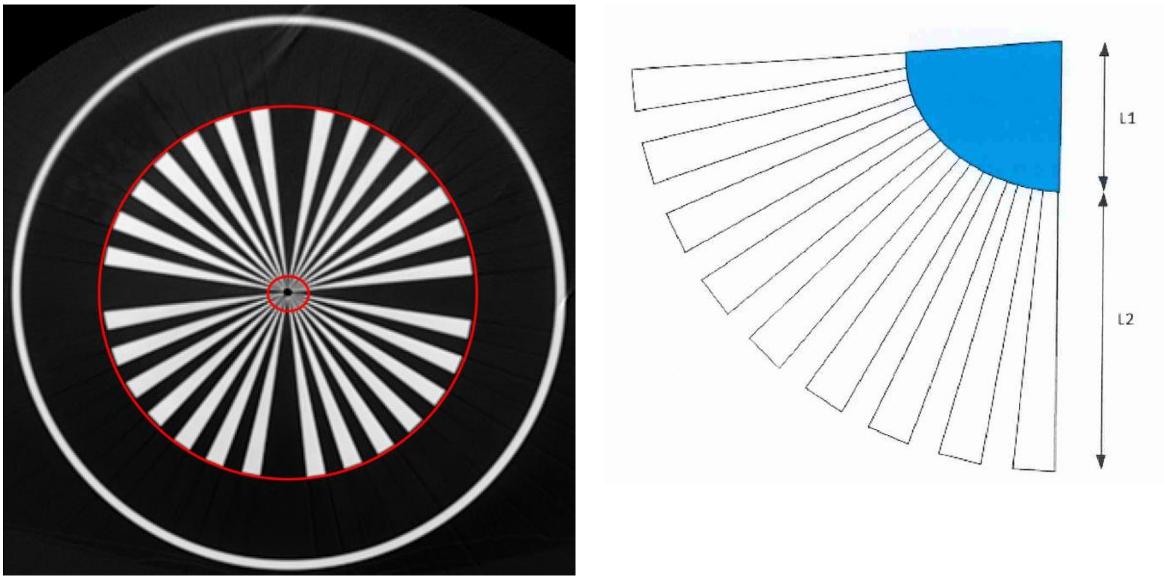

Figure 4. The spatial resolution test uses Perspex elements separated by 10mm at their outer edge, and tapering to a point where they meet in the centre of the circle shown (a). The blue region represented in (b) represents the area where the bars can no longer be observed. This length is represented by the formula L1 = 100mm-L2

Grid resolution test

The grid resolution test (Figure 5) is somewhat similar to the spatial resolution test, although more qualitative in its interpretation. Slots of 1mm to 6mm thickness are visualised in the CT image, and the smallest size that can be resolved indicates resolution.

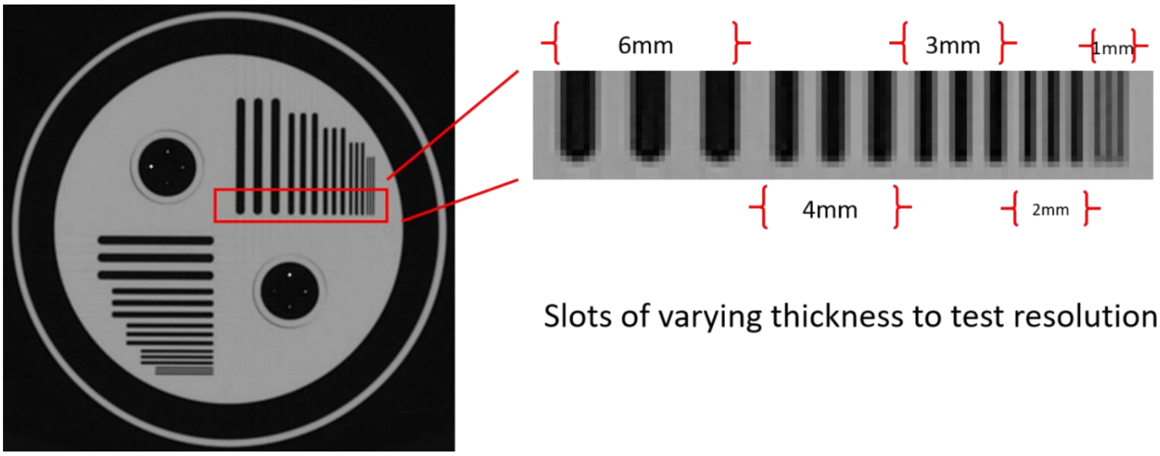

Figure 5. The grid resolution test showing slots cut into Perspex that are separated by between 1mm to 6mm.

Density test

The density test uses a series of rods inserted into Perspex. These rods are selected to provide a variety of densities in the organic range, with cross-sectional scans captured both within the Perspex where the rods are completely surrounded by Perspex (see right side image in Figure 6), and also where they extrude from the Perspex and are therefore surrounded by air (see left side image in Figure 6). In this case the average Hu value of the pixels depicting each of the rods was determined. These rods and their corresponding densities included polypropylene (0.91 g/cm^3), acrylonitrile butadiene styrene (1.0 g/cm^3), polycarbonate (1.1 g/cm^3), peek (1.3 g/cm^3), Delrin (1.4 g/cm^3), chlorinated PVC (1.5 g/cm^3), polyvinylidene fluoride (1.75 g/cm^3), Teflon (2.2 g/cm^3), and the scattering plate consisted of Perspex (1.2 g/cm^3).

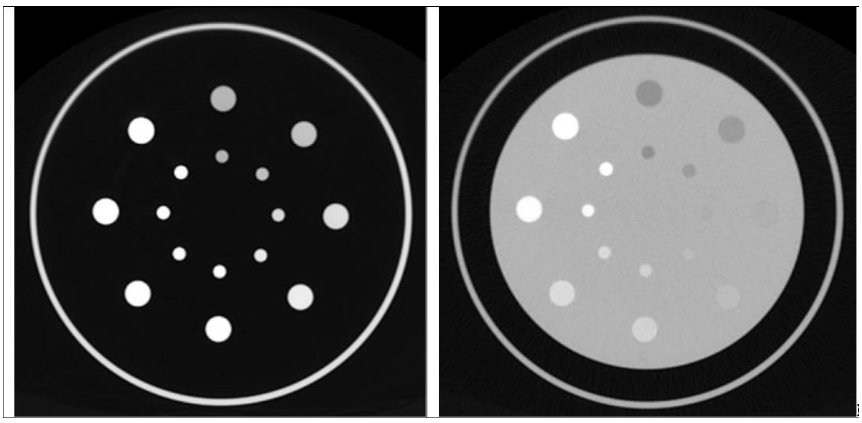

Figure 6. The density test showing rods embedded in Perspex (on the right) and rods extending out of Perspex and surrounded by air (on the left).

3.6 Statistical analysis

RTT-110 determined lean, fat and bone % values were analysed using general linear models (SAS) for their ability to predict medical CT lean, fat and bone % of each primal or lamb section. In beef, assessing the precision of Rapiscan prediction of CT composition allowed the optimal tissue thresholds to be determined for Rapiscan images and thus the optimal precision with which Rapiscan RTT-110 scans can predict CT lean, fat, and bone%.

For assessment of the XTE-CT test piece, where quantitative values were available, these were pooled across the 5 scans taken on the RTT110. The mean, standard deviation, minimum, and maximum values across these 5 scans was then reported. This process was repeated for the 5 medical CT scans of this test piece.

4. Results

4.1 Beef primals

Fat, lean and bone tissue could be reasonably well differentiated on qualitative assessment of RTT-110 images of beef short loins and rib sets. This can be seen in the example image slices shown in Tables 4 and 5, where the equivalent medical CT image slice of the same primal is shown alongside as a direct comparison. Even muscle seams can be visually identified in Rapiscan images, though not with the same clarity as in medical CT images (Tables 4 and 5).

To assess the differentiation of tissue types within images, example frequency plots of pixel values are shown in Tables 4 and 5 for a number of short loins and rib sets. In medical CT images these frequency distributions show the expected differentiation of fat and lean tissue, with separate peaks at about -60 and +60 Hounsfield unit values aligning with fat and muscle tissue, and the bone pixel values being distributed above this level. The frequency distributions of Rapiscan image pixel values also demonstrated some separation into pixel value peaks corresponding to fat and lean tissue. However, the values and extent of these peaks were less consistent between different primals (Tables 4 and 5) and even between the different image slices of the same primal.

The precision with which different fat to lean thresholds in RTT-110 images could predict CT fat and lean % are shown in Table 2. A fat:lean threshold pixel value of 760 produced the most precise prediction of CT lean and fat%, though only very minor differences in precision were observed in rib sets. Similarly, only very small shifts in precision were seen with variation in the lean:bone threshold between 1000 and 1040 (Table 3), with thresholds of 1010 to 1020 producing the best predictions of CT composition.

Table 2. The precision (R-squared and root mean square error or RMSE) of Rapiscan RTT-110 fat:lean pixel value thresholds predicting CT fat and lean % of beef short loins and rib sets. A lean:bone pixel threshold of 1020 was consistently applied in this analysis of Rapiscan images.

	Short loins				Rib sets			
Rapiscan fat to lean threshold	CT fat %		CT lean %		CT fat %		CT lean %	
	R^2	RMSE	R^2	RMSE	R^2	RMSE	R^2	RMSE
740	0.69	2.94	0.31	3.87	0.02	3.51	0.04	3.07
760	0.74	2.70	0.42	3.55	0.035	3.48	0.02	3.10
780	0.69	2.95	0.42	3.55	0.035	3.48	0.006	3.12
800	0.49	3.76	0.31	3.86	0.03	3.49	0.002	3.13
820	0.22	4.64	0.18	4.23	0.03	3.48	0.0005	3.13
840	0.085	5.04	0.09	4.45	0.05	3.46	0.0006	3.13

Table 3. The precision (R-squared and root mean square error or RMSE) of Rapiscan RTT-110 lean:bone pixel value thresholds predicting CT lean and bone % of beef short loins and rib sets. A fat:lean pixel threshold of 760 was consistently applied in this analysis of Rapiscan images.

	Short loins				Rib sets			
Rapiscan lean to bone threshold	CT lean %		CT bone %		CT lean %		CT bone %	
	R^2	RMSE	R^2	RMSE	R^2	RMSE	R^2	RMSE
1000	0.46	3.42	0.96	0.66	0.015	3.11	0.53	1.14
1010	0.43	3.51	0.98	0.52	0.016	3.11	0.54	1.13
1020	0.42	3.55	0.98	0.51	0.018	3.10	0.53	1.14
1030	0.42	3.56	0.98	0.46	0.019	3.11	0.38	2.79
1040	0.42	3.55	0.98	0.48	0.020	3.10	0.50	1.18

Rapiscan prediction of CT fat, lean and bone % in beef short loins and rib sets using Rapiscan thresholds of 300 to 760 for fat; 760 to 1020 for lean and greater than 1020 for bone are shown in Fig. 5. RTT-110 scans predicted CT bone % in short loins with excellent precision, though could only predict CT bone % in rib sets with moderate precision (Fig. 5). RTT-110 scans predicted CT fat % in short loins with good precision, though CT fat % was poorly predicted in rib sets. Similarly, primal CT lean % was predicted moderately by Rapiscan scans in short loins, but poorly in beef rib sets (Fig. 5).

Images demonstrating how these thresholds differentiate tissue types in Rapiscan images are shown in Tables 4 and 5, along with the corresponding medical CT image of each primal cross-section with tissue differentiation using established thresholds.

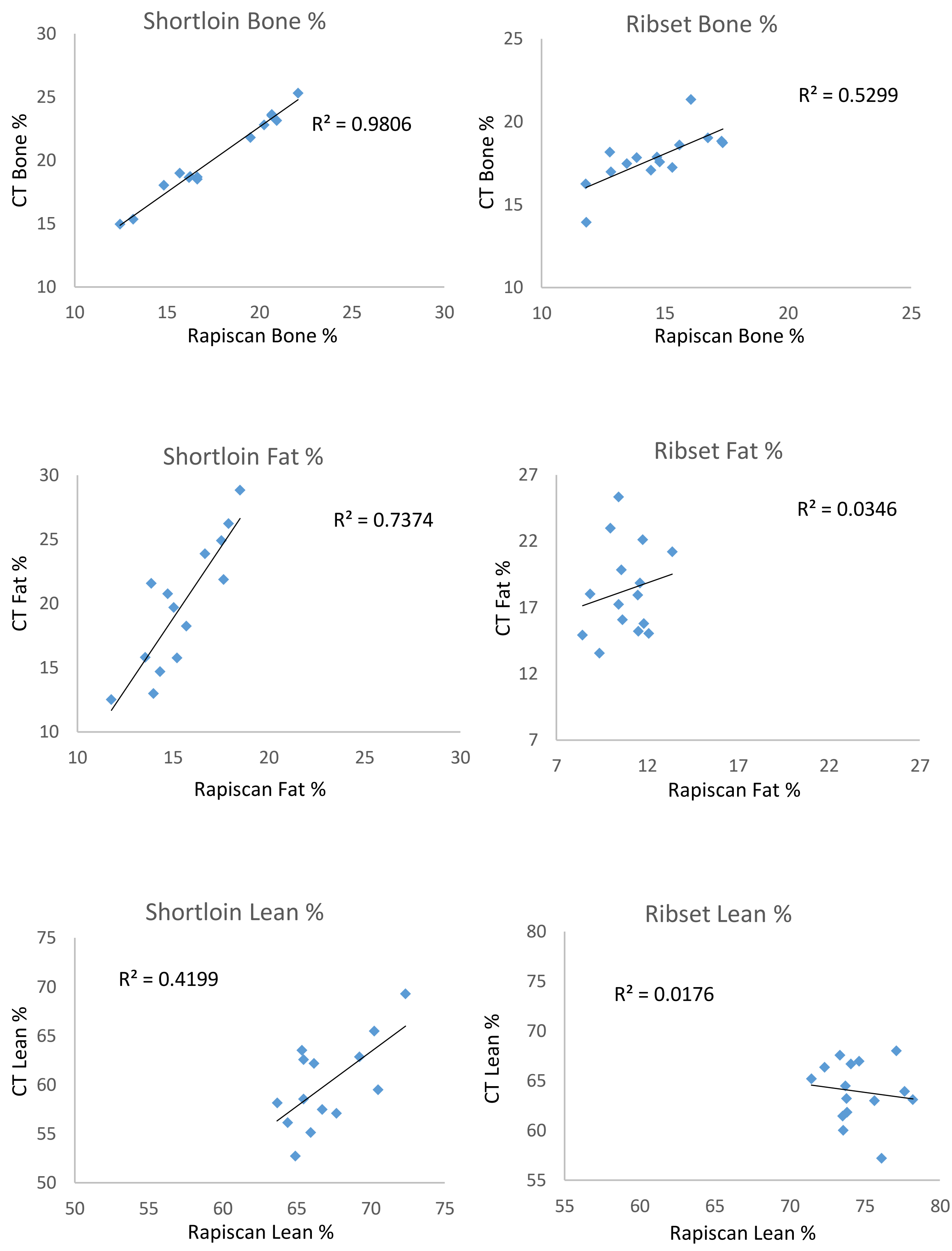

Figure 5. The relationships between Rapiscan and medical CT estimates of bone, fat and lean % in beef short loins and ribsets. Points represent individual beef primal estimates; the line represents the line of best fit while the R^2 and root mean square error (RMSE) demonstrate the precision of each prediction.

Table 4. Example medical CT and Rapiscan RTT-110 image slices of the same anatomical site in four short loin primals sourced from carcases phenotypically diverse in weight and fatness. Frequency distributions of pixel values within the selected image slices are shown, in addition to images demonstrating the thresholding of fat, lean and bone tissue in the selected slices.

	Medical CT	Rapiscan
	Short loin number 4	
	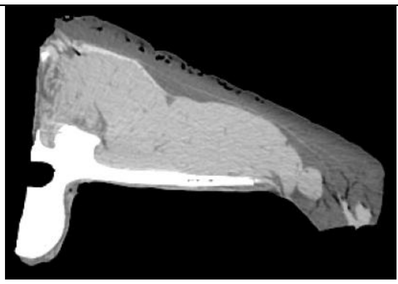 Slice 749	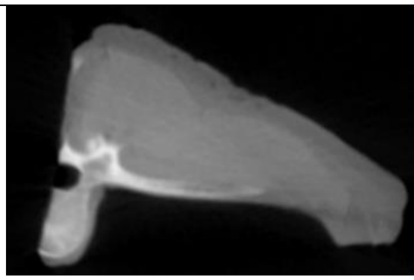 Slice 265
Pixel count	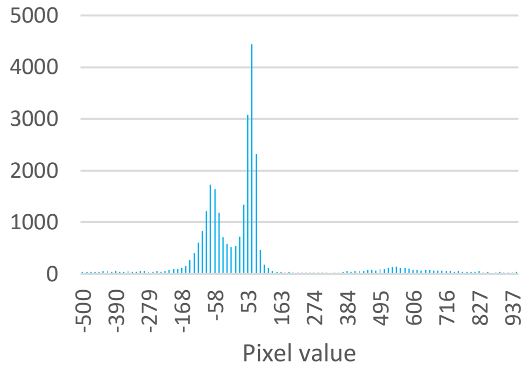	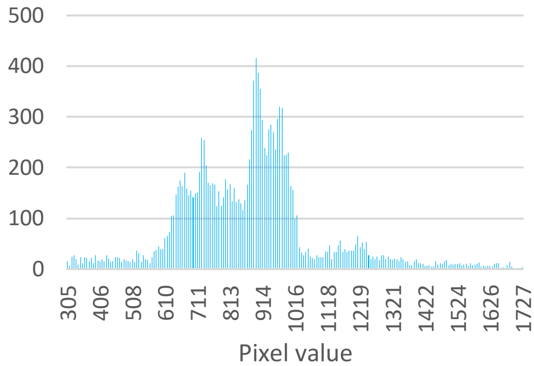
Tissue thresholding	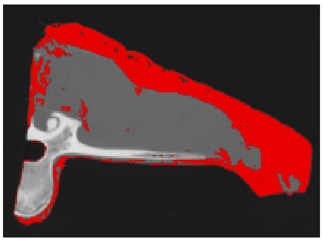 Fat (-235 – 2)	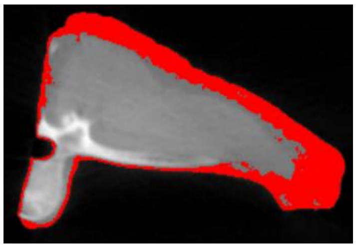 Fat (300 – 760)
	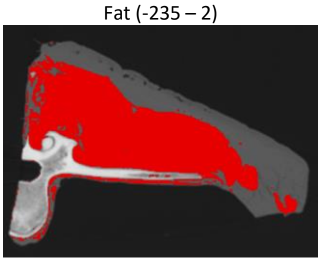 Lean (2 – 164)	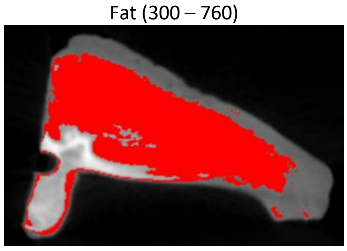 Lean (760 – 1020)
	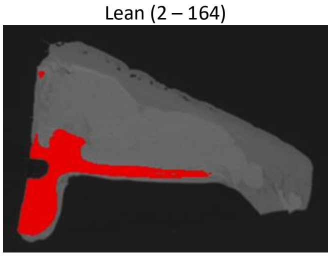 Bone (164 – 32767)	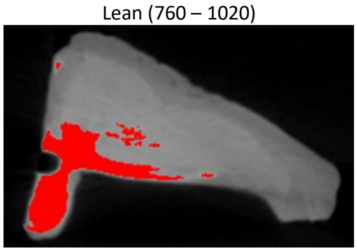 Bone (1020 – 65535)
	Short loin number 9	

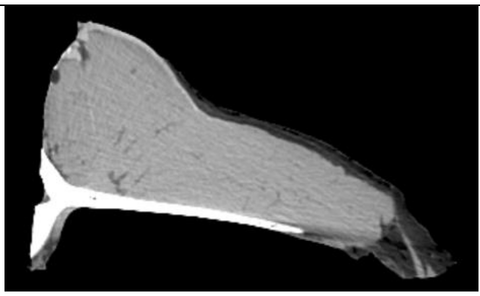

Slice 761

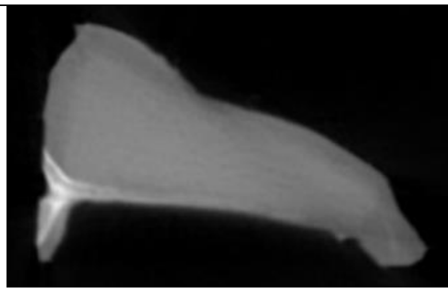

Slice 255

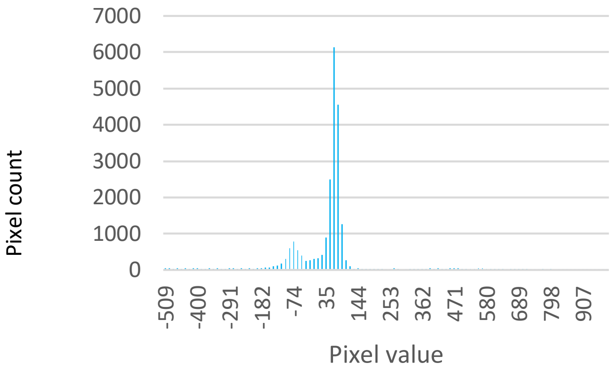

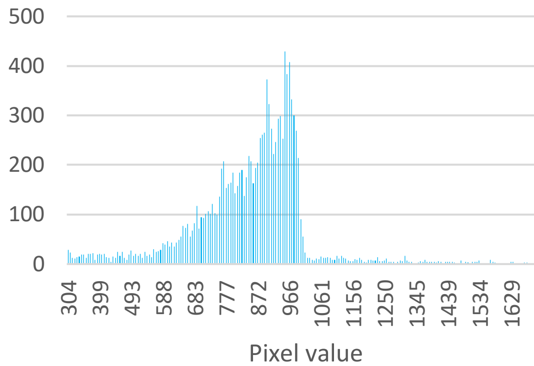

Tissue thresholding

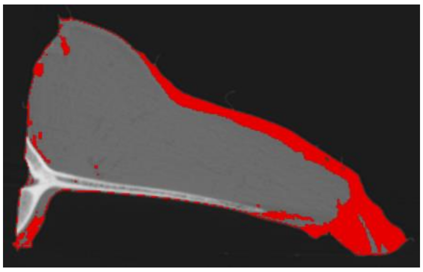

Fat (-235 – 2)

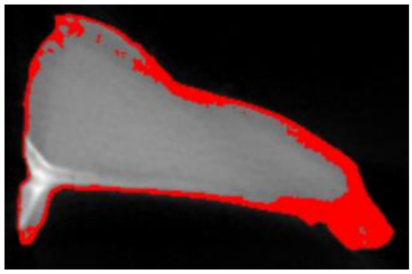

Fat (300 – 760)

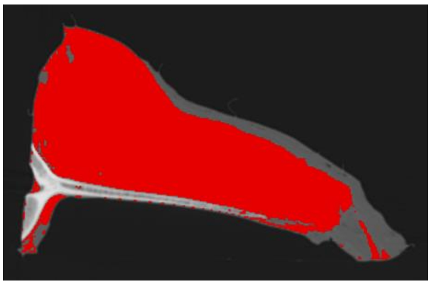

Lean (2 – 164)

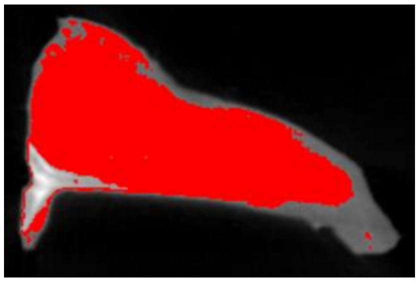

Lean (760 – 1020)

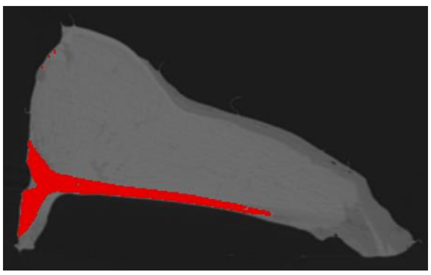

Bone (164 – 32767)

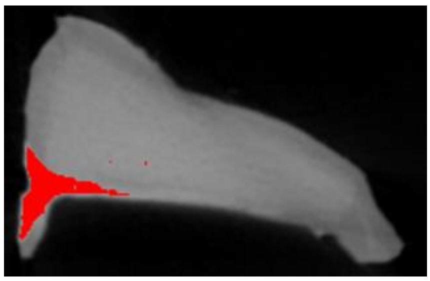

Bone (1020 – 65535)

Short loin number 11

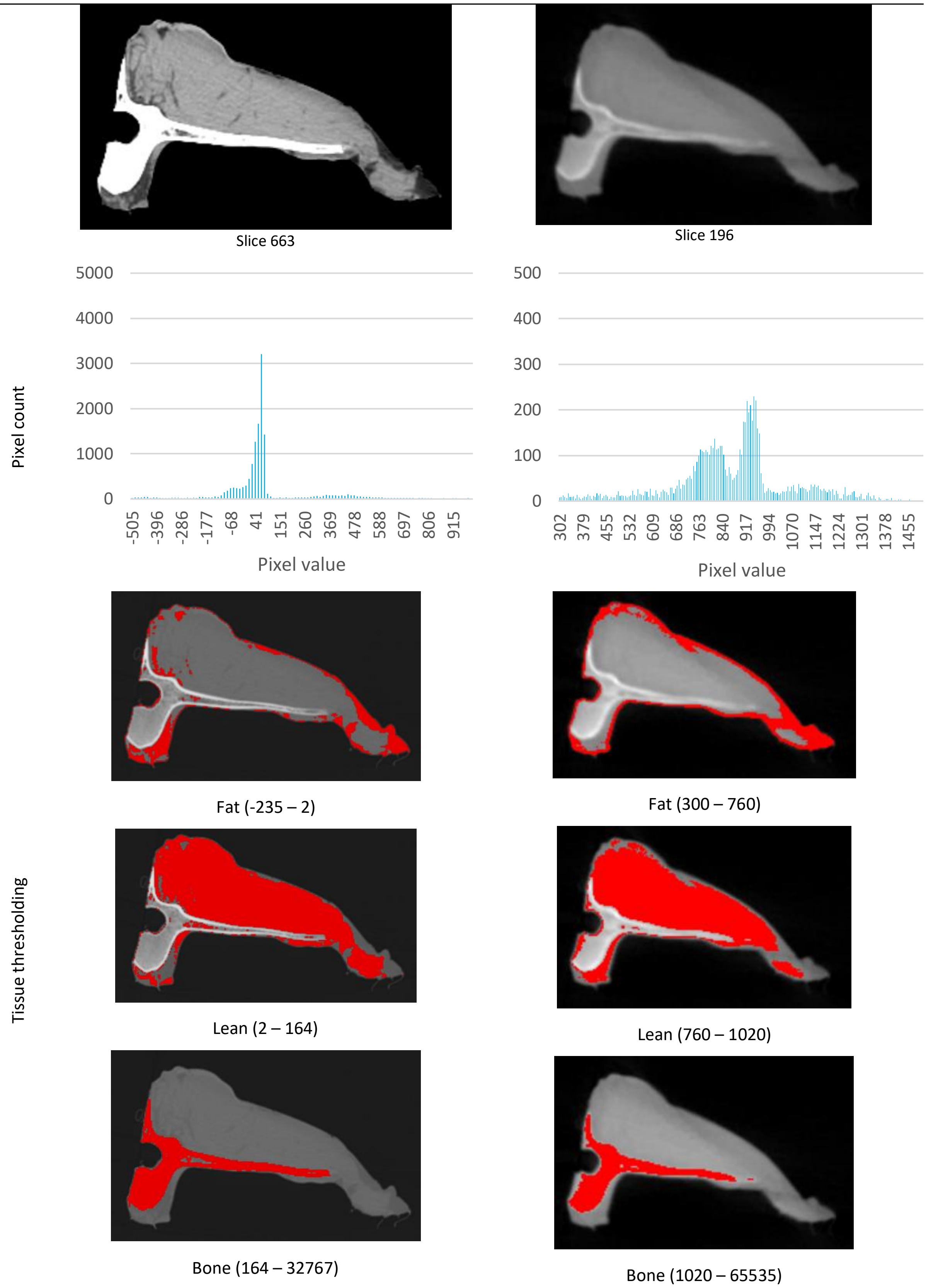

Short loin number 14

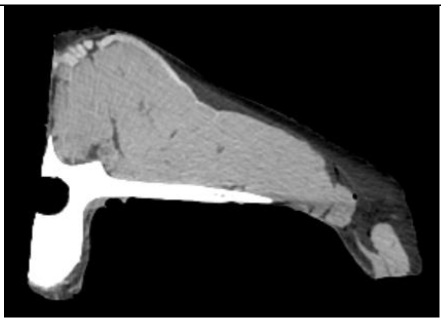

Slice 677

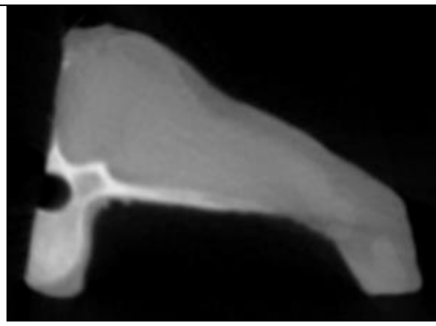

Slice 239

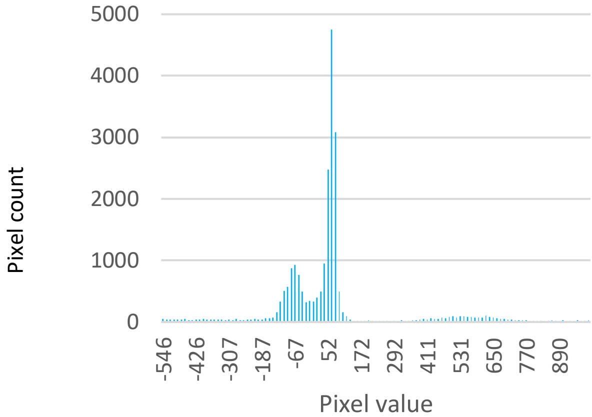

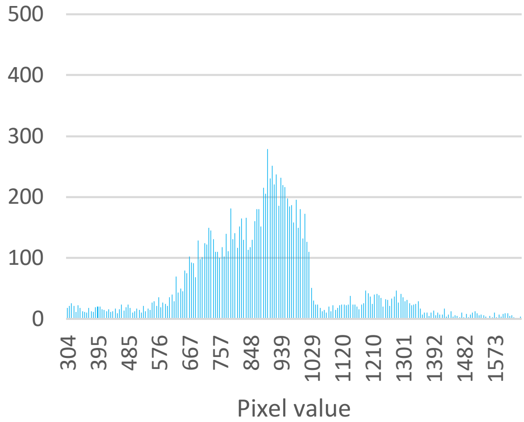

Tissue thresholding

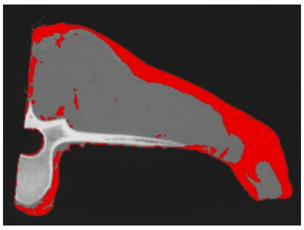

Fat (-235 – 2)

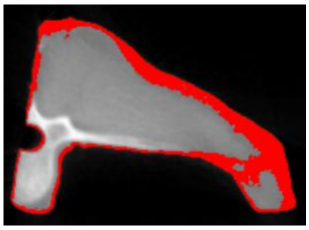

Fat (300 – 760)

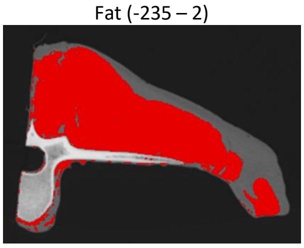

Lean (2 – 164)

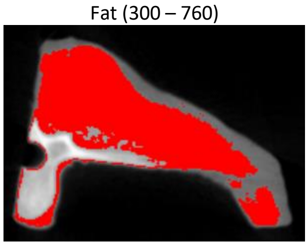

Lean (760 – 1020)

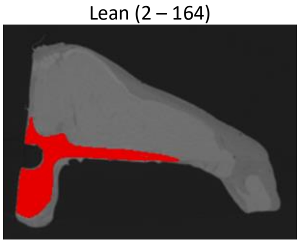

Bone (164 – 32767)

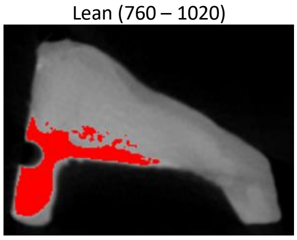

Bone (1020 – 65535)

Table 5. Example medical CT and Rapiscan RTT-110 image slices of the same anatomical site in four rib set primals sourced from carcasses phenotypically diverse in weight and fatness. Frequency distributions of pixel values within the selected image slices are shown, in addition to images demonstrating the thresholding of fat, lean and bone tissue in the selected slices.

	Medical CT	Rapiscan RTT-110
	Rib set number 4	
	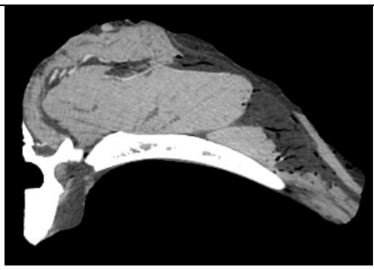 Slice 355	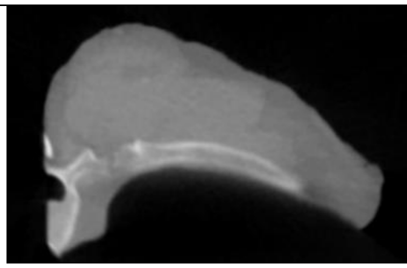 Slice 355
	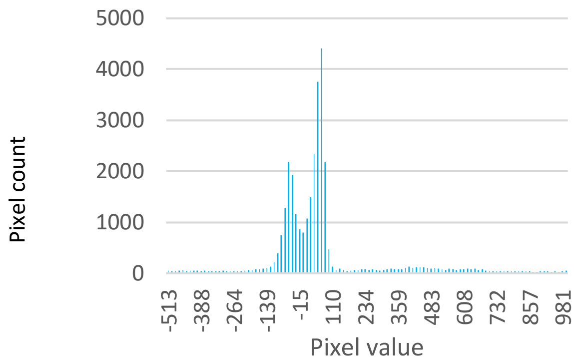	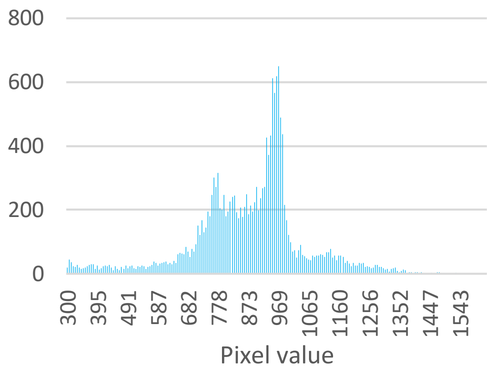
Tissue thresholding	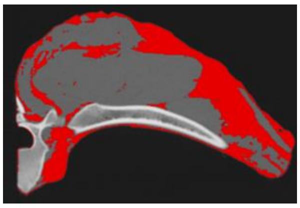 Fat (-235 – 2)	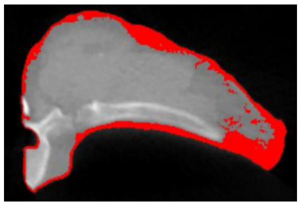 Fat (300 – 760)
	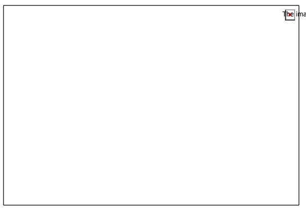 Lean (2 – 164)	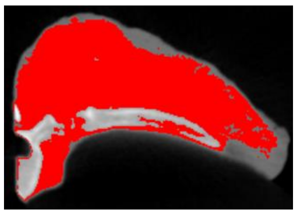 Lean (760 – 1020)
	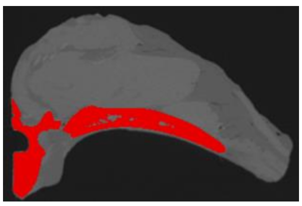 Bone (164 – 32767)	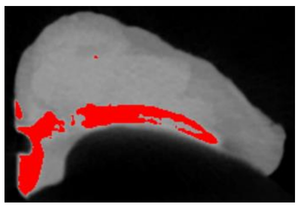 Bone (1020 – 65535)
	Ribset number 9	

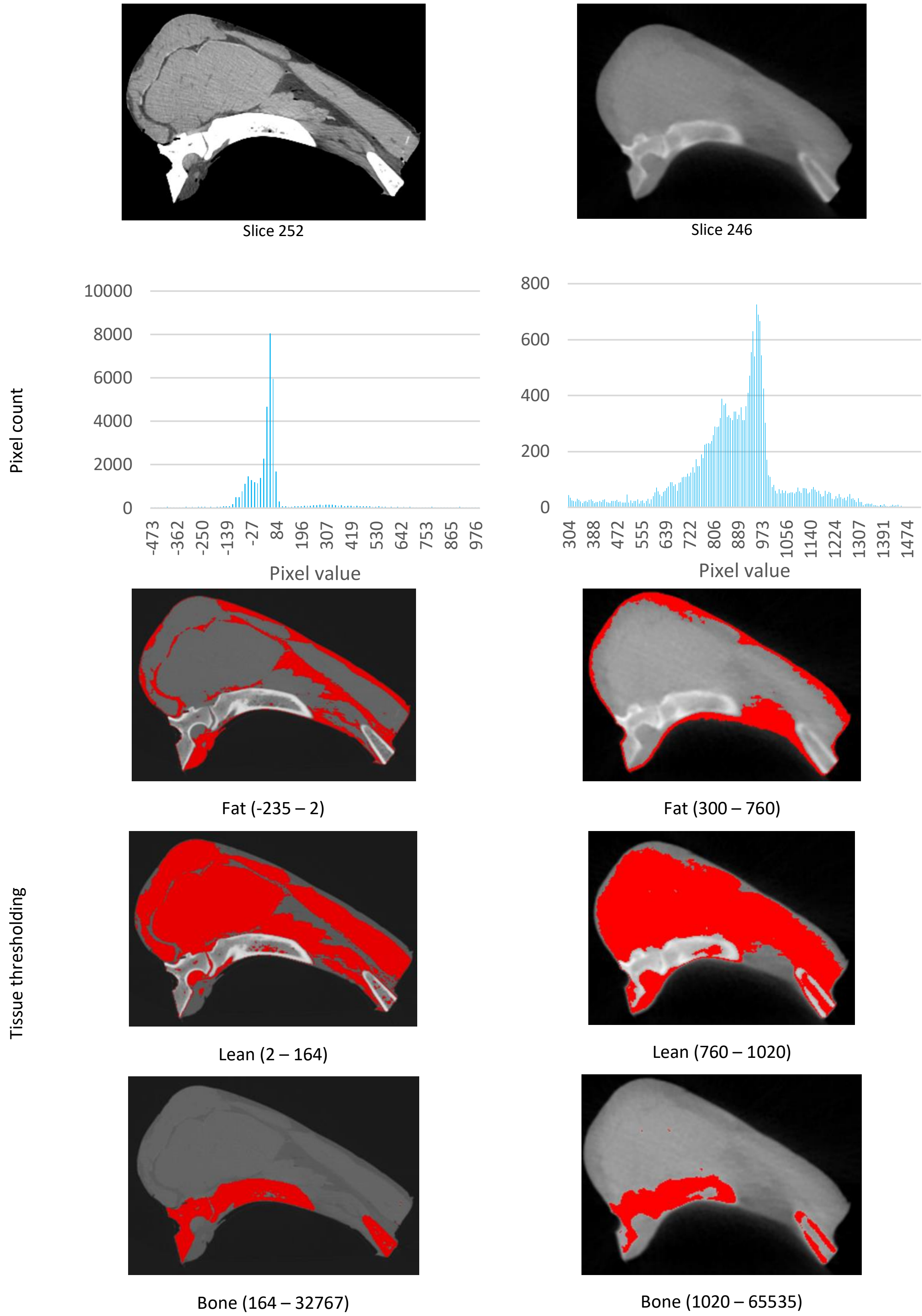

Ribset number 11

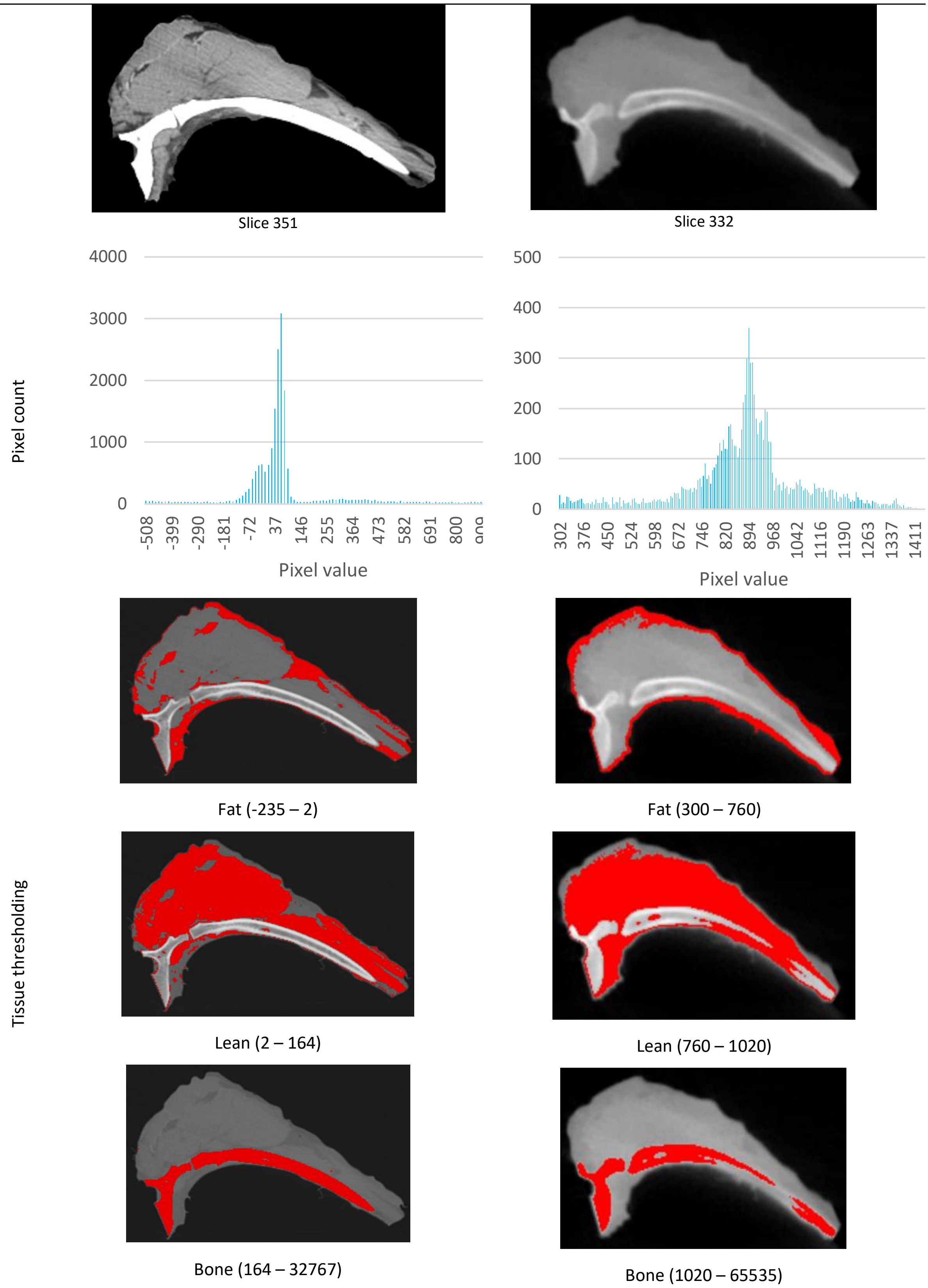

Ribset number 14

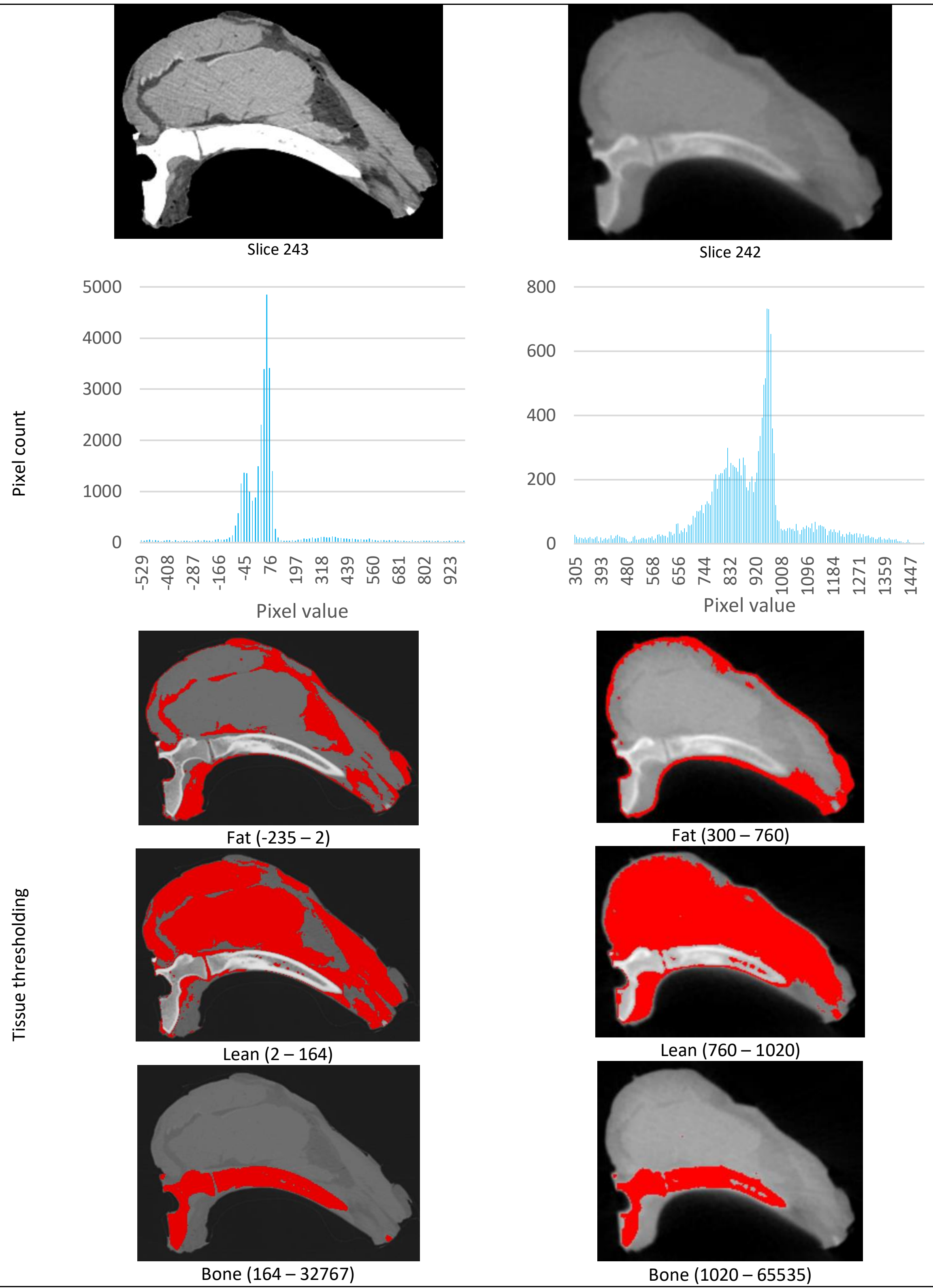
Slice 243
Slice 242
Pixel count
5000
4000
3000
2000
1000
0
-529
-408
-287
-166
-45
76
197
318
439
560
681
802
923
Pixel value
800
600
400
200
0
305
393
480
568
656
744
832
920
1008
1096
1184
1271
1359
1447
Pixel value
Tissue thresholding
Fat (-235 – 2)
Fat (300 – 760)
Lean (2 – 164)
Lean (760 – 1020)
Bone (164 – 32767)
Bone (1020 – 65535)

4.2 Lamb carcases

Similar to beef, different tissue types could be well differentiated on visual or qualitative assessment of RTT-110 images of lamb carcases. This can be seen in the example image slices shown in Tables 7, 8 and 9, where the approximate equivalent medical CT image slice of the same section is shown alongside as a direct comparison. However, the shape of lamb sections make their positioning through the RTT-110 and medical CT system less consistent than beef primals and therefore it is more difficult to compare the exact same slice or image of lamb sections through the two systems. Muscle seams can also be visually identified in Rapiscan images, though not with the same clarity as in medical CT images (Tables 7, 8 and 9).

Example frequency plots of pixel values are shown for the fore (Table 7), saddle (Table 8) and hind section (Table 9) to demonstrate the ability the differentiation of tissue types within images based on pixel values. As in beef images, the frequency distributions of lamb medical CT images show the expected differentiation of fat and lean tissue, with separate peaks at about -60 and +60 Hounsfield unit, and bone pixels above this level. However, the frequency distributions of Rapiscan image pixel values were even more inconsistent in lamb than beef, with the rough peaks corresponding to fat and lean tissue differing between carcasses and within a section.

The precision of RTT-110 image prediction of CT fat, lean and bone % in lamb fore, saddle and hind sections are shown in Table 6. RTT-110 scans predicted CT bone % with excellent precision and CT fat and lean % with good precision.

Table 6. The precision (R-squared and root mean square error or RMSE) of Rapiscan RTT-110 predicting CT fat, lean, and bone % in the fore, saddle and hind sections of lamb.

Lamb section	CT fat %		CT lean %		CT bone %	
	R^2	RMSE	R^2	RMSE	R^2	RMSE
Fore section	0.75	3.64	0.64	3.04	0.86	1.11
Saddle	0.83	2.15	0.57	2.38	0.95	0.55
Hind section	0.72	2.82	0.57	2.57	0.94	0.48

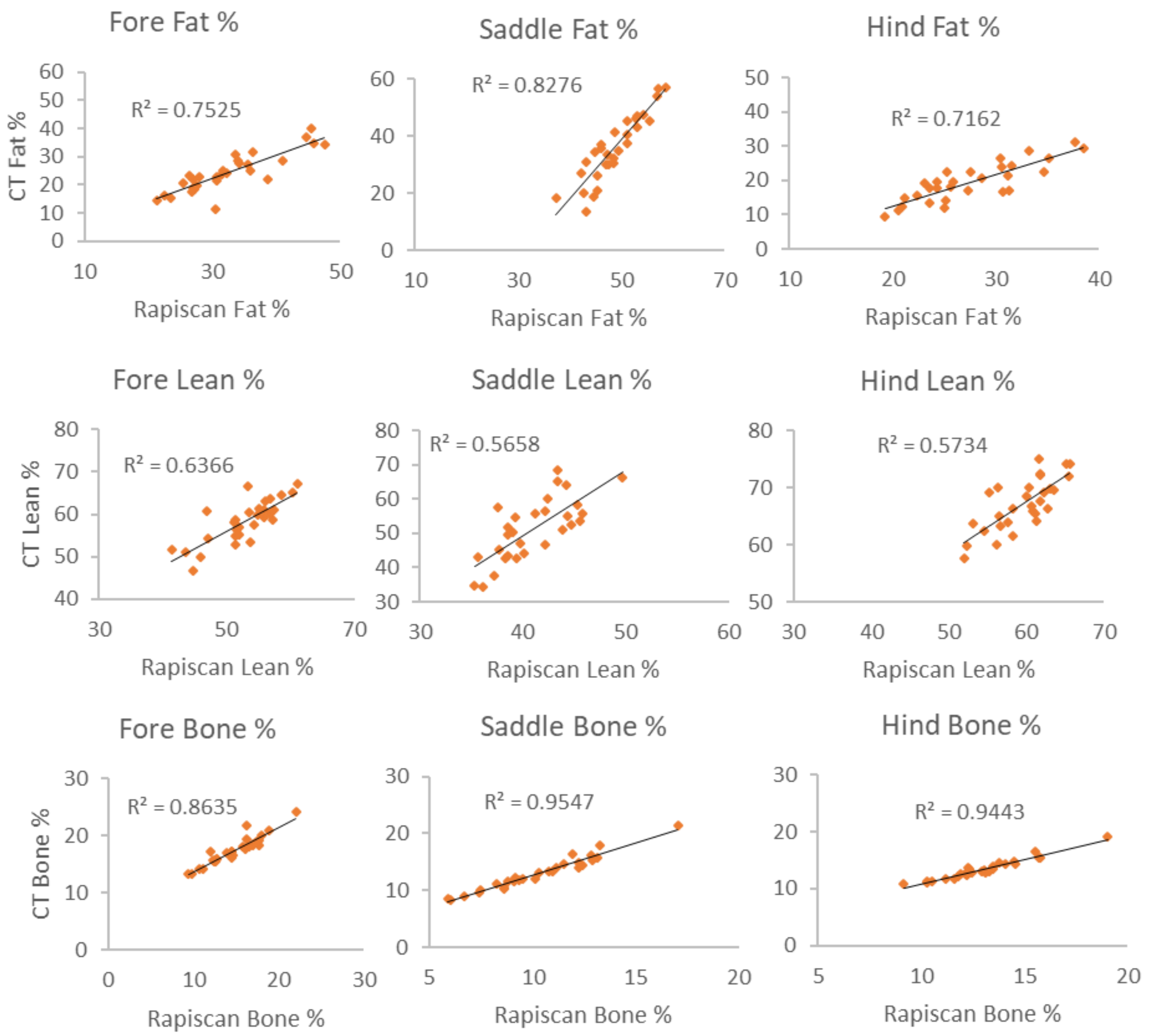

Figure 6. The relationships between Rapiscan and medical CT estimates of bone, fat and lean % in lamb fore, saddle and hind sections. Points represent individual lamb section estimates; the line represents the line of best fit while the R^2 and root mean square error (RMSE) demonstrate the precision of each prediction.

Examples of fat, lean and bone tissue differentiation via pixel value thresholding in RTT-110 and medical CT images of lamb fore, saddle and hind sections are shown in Tables 7, 8 and 9. In Rapiscan RTT-110 images thresholds of -250 to -50 have been used to identify fat tissue; -50 to 125 for lean and > 125 to identify bone tissue. A particularly lean lamb carcase (number 7, 13.5 kg and 3 mm GR tissue depth) and a particularly fat lamb carcase (number 29: 29.9 kg and 31 mm GR tissue depth) have been chosen as examples in Tables 7 to 9.

Table 7. Example medical CT and Rapiscan RTT-110 image slices of similar anatomical sites in two fore sections sourced from two carcases phenotypically diverse in weight and fatness. Frequency distributions of pixel values within the selected image slices are shown, in addition to images demonstrating the thresholding of fat, lean and bone tissue in the selected slices.

	Medical CT	Rapiscan
	Fore section number 7	
		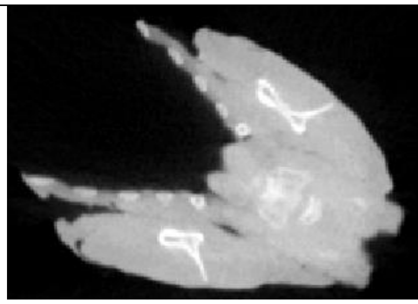
Pixel count	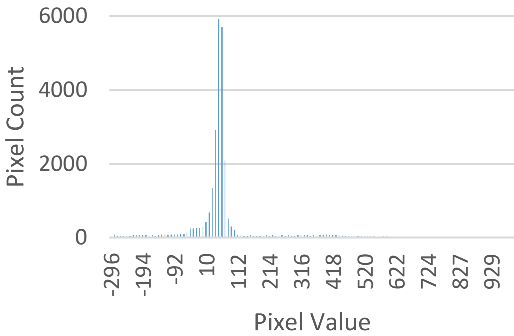	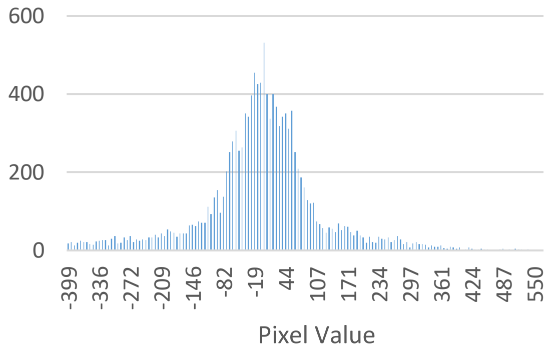
Tissue thresholding	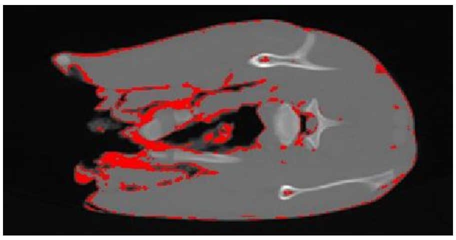 Fat (-235 to 2)	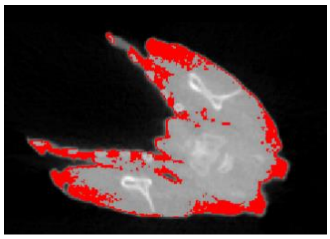 Fat (-250 to -50)
	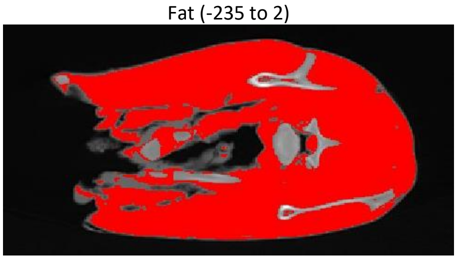 Lean (2 to 164)	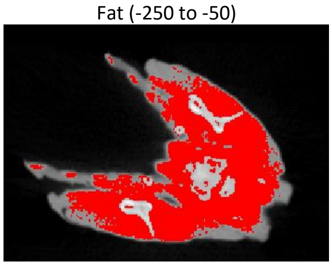 Lean (-50 to 125)
	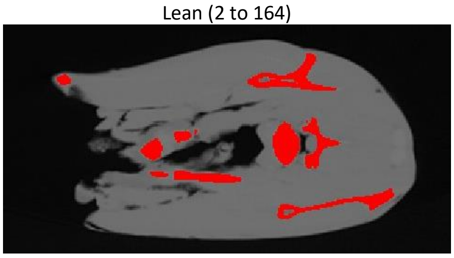 Bone (164 to 32767)	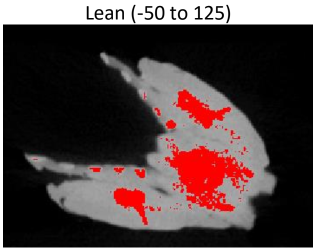 Bone (greater than 125)
	Fore section number 29	

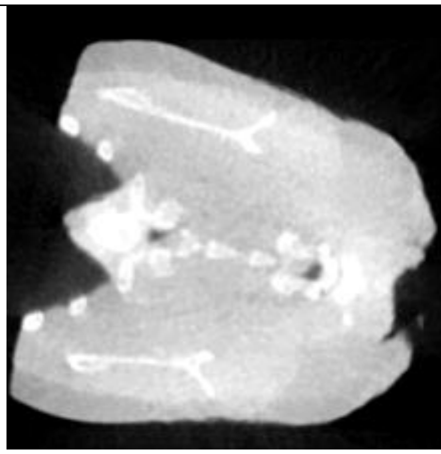

Pixel count

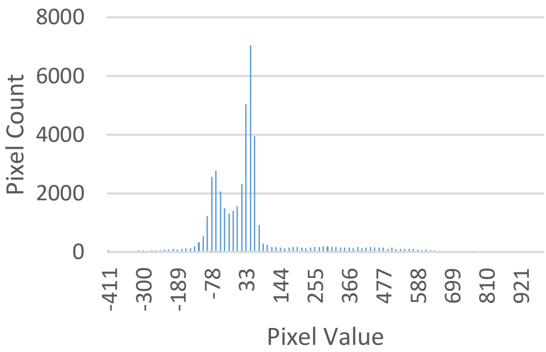

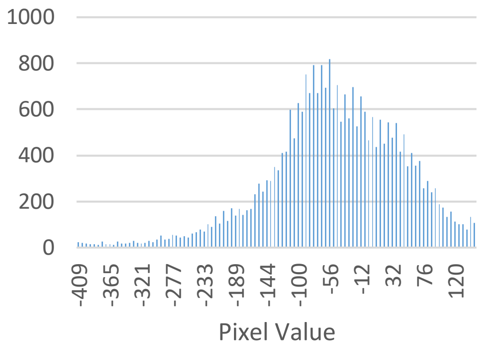

Tissue thresholding

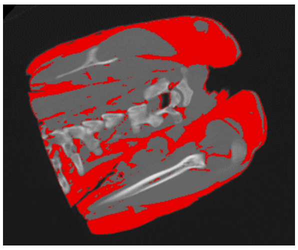

Fat (-235 to 2)

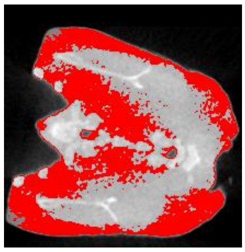

Fat (-250 to -50)

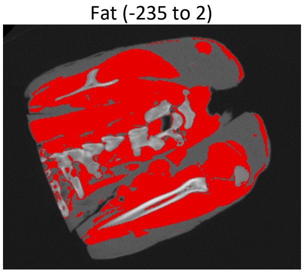

Lean (2 to 164)

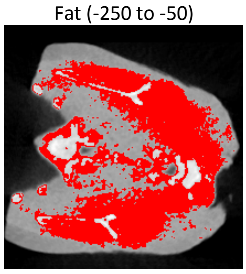

Lean (-50 to 125)

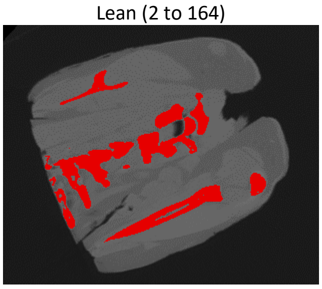

Bone (164 to 32767)

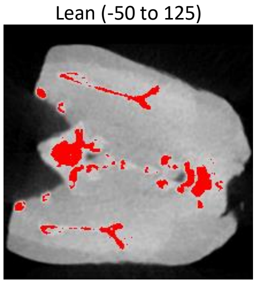

Bone (greater than 125)

Table 8. Example medical CT and Rapiscan RTT-110 image slices of similar anatomical sites in two saddle sections sourced from carcases phenotypically diverse in weight and fatness. Frequency distributions of pixel values within the selected image slices are shown, in addition to images demonstrating the thresholding of fat, lean and bone tissue in the selected slices.

Saddle number 7

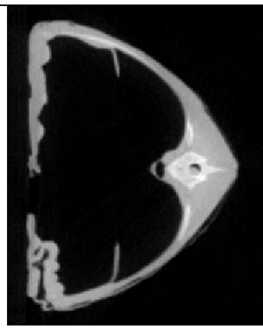

Pixel count

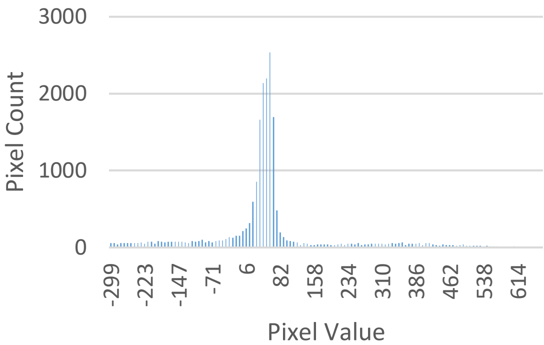

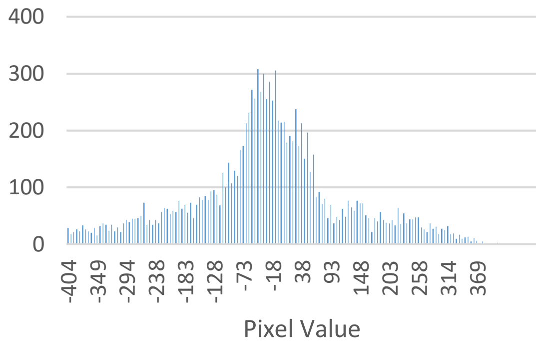

Tissue thresholding

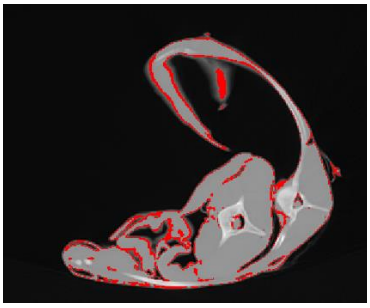

Fat (-235 to 2)

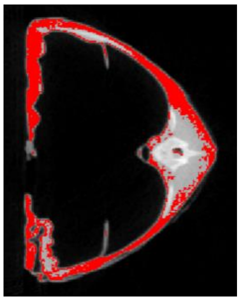

Fat (-250 to -50)

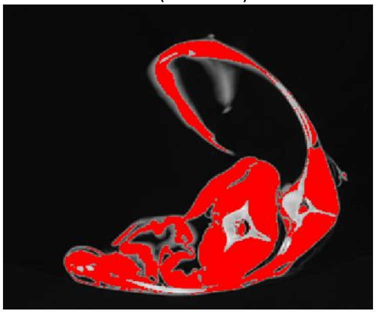

Lean (2 to 164)

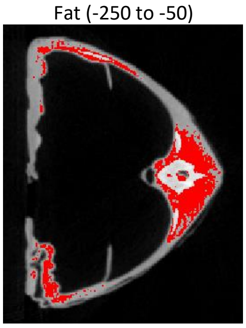

Lean (-50 to 125)

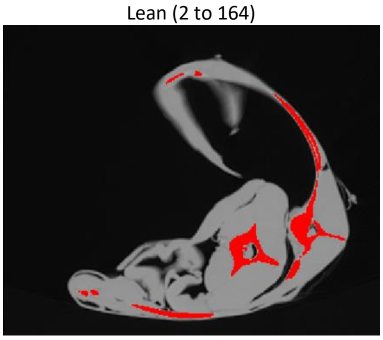

Bone (164 to 32767)

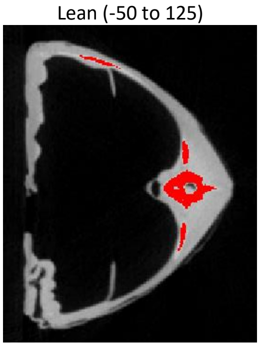

Bone (greater than 125)

Saddle number 29

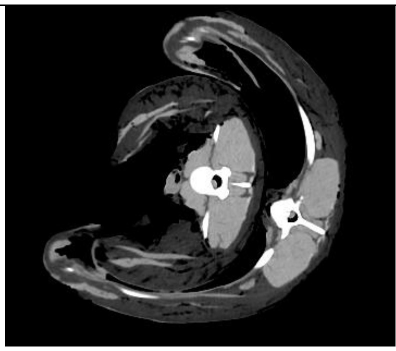

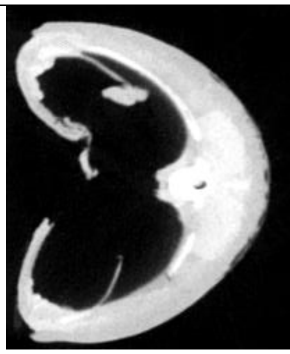

Pixel count

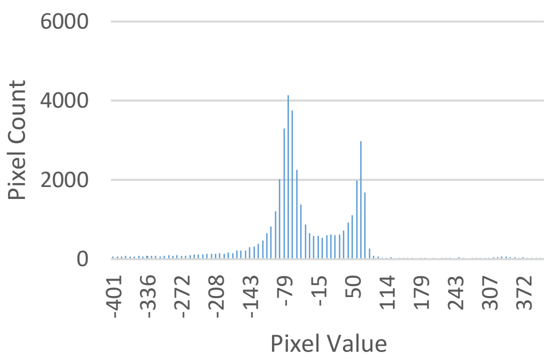

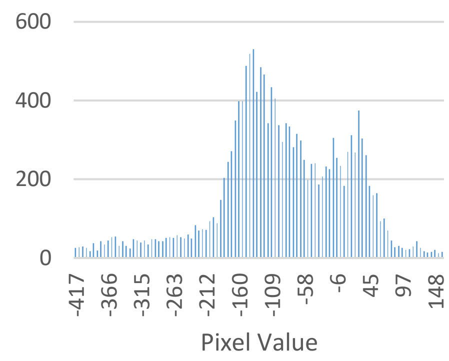

Tissue thresholding

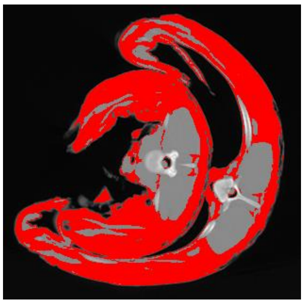
Fat (-235 to 2)

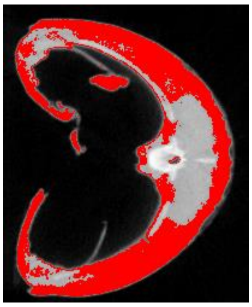
Fat (-250 to -50)

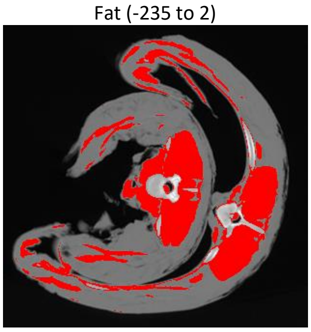
Lean (2 to 164)

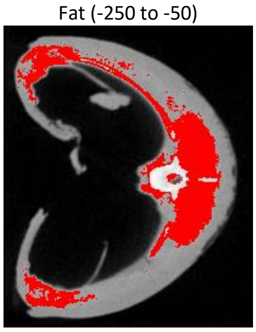
Lean (-50 to 125)

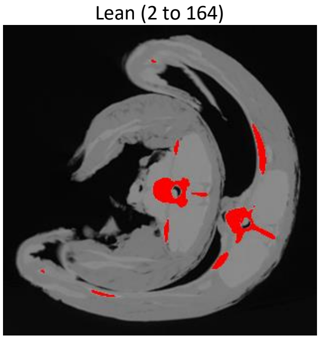
Bone (164 to 32767)

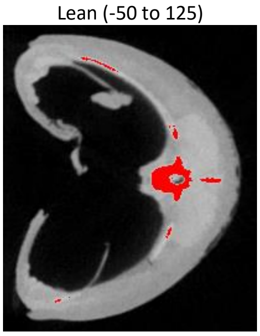
Bone (greater than 125)

Table 9. Example medical CT and Rapiscan RTT-110 image slices of similar anatomical sites in two hind sections sourced from carcases phenotypically diverse in weight and fatness. Frequency distributions of pixel values within the selected image slices are shown, in addition to images demonstrating the thresholding of fat, lean and bone tissue in the selected slices.

Hind section number 7

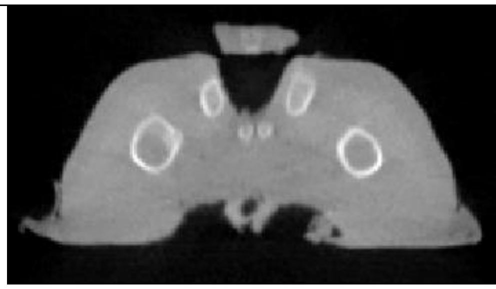

Pixel count

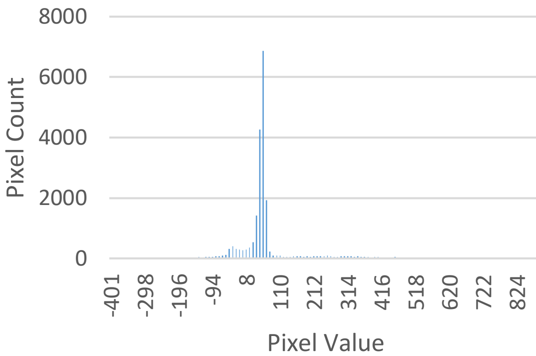

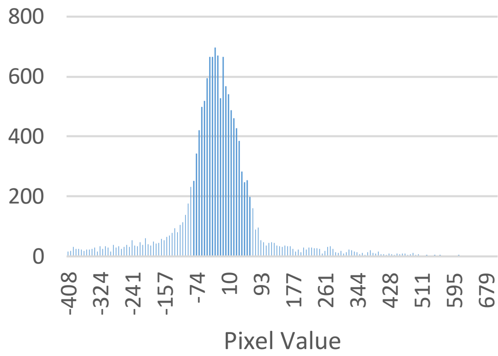

Tissue thresholding

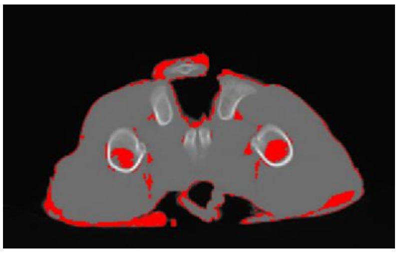

Fat (-235 to 2)

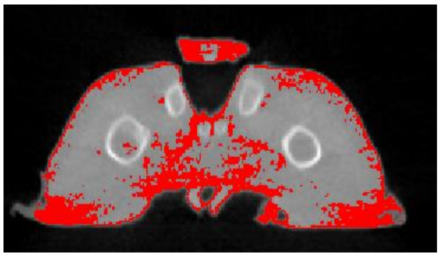

Fat (-250 to -50)

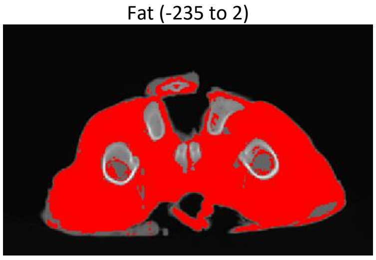

Lean (2 to 164)

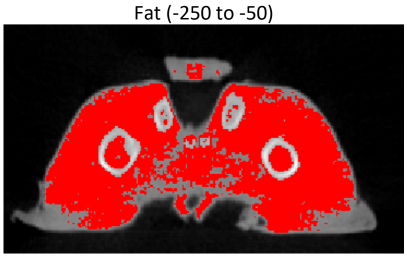

Lean (-50 to 125)

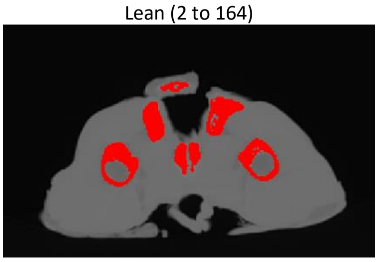

Bone (164 to 32767)

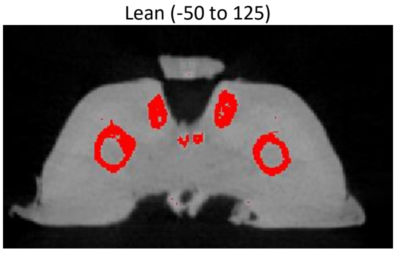

Bone (greater than 125)

Hind section number 29

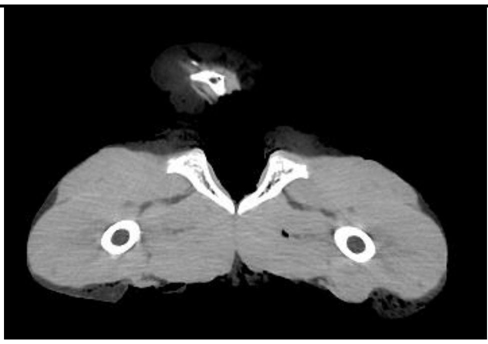

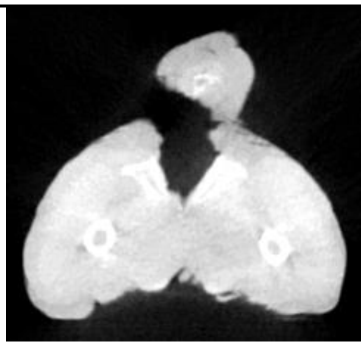

Pixel count

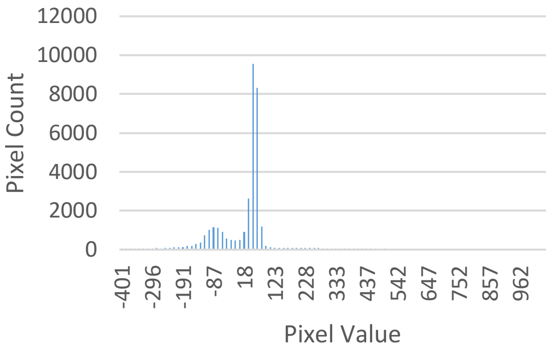

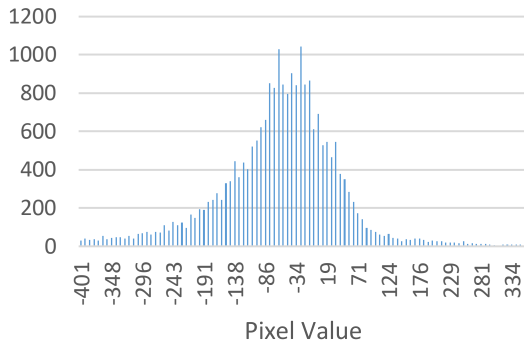

Tissue thresholding

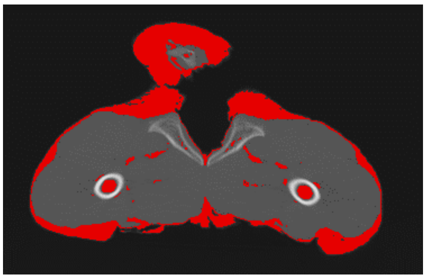

Fat (-235 to 2)

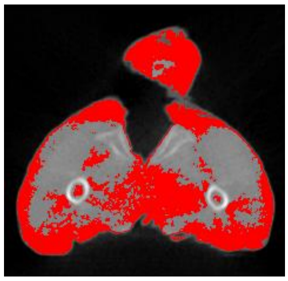

Fat (-250 to -50)

Lean (2 to 164)

Lean (-50 to 125)

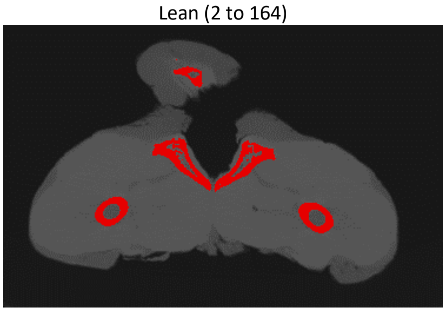

Bone (164 to 32767)

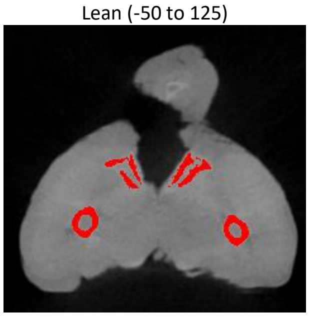

Bone (greater than 125)

4.3 Calibration device analysis

The RTT-110 demonstrated resolution that approached that of the medical CT scanner used in this study. This was demonstrated by the grid resolution test (**Figure 7**) which showed differentiation of the 2mm sections although not the 1mm sections, and the spatial resolution test (see Table 10) in which the resolution was calculated to be 1.54mm (see Table 12). In comparison, the medical CT scanner showed differentiation of 1mm sections within the grid resolution test (**Figure 7**), and a calculated resolution of 1.0mm in the spatial resolution test (see Table 12). For both CT scanners these values varied little across the 5 scans of the XTE-CT test piece.

Simple dimension measurements for both scanners were highly precise, although the RTT-110 demonstrated inaccuracy likely reflecting the need for scale calibration. This was demonstrated by the diameter measurement of the 200mm section which was measured with excellent repeatability across both scanners, although measured inaccurately on the RTT-110, with average values of only 169mm contrasting with 201mm measured using the medical CT scanner (Table 12). Alternatively, the thickness measurement based upon the count of 1mm slice widths was accurate and repeatable across both scanners (Table 12).

The density analysis of different materials demonstrated marked differences in reported Hu values for these materials, but also marked differences between the RTT-110 versus the medical CT scanner (Table 11). This reflects that the RTT-110 is calibrated across a different Hu value range compared to the medical CT. It was also notable that the medical CT scanner demonstrated variation in the pixel values for each substance, yet this variation was greater by at least twice in the RTT-110 scanner.

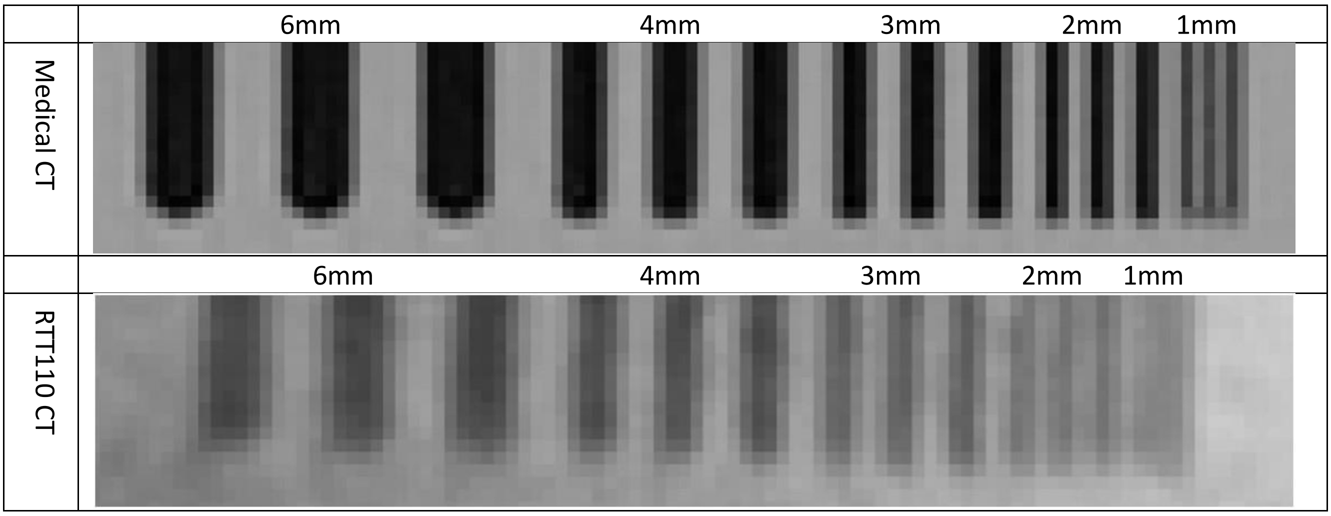

Figure 7. Grid resolution test for the medical CT and the RTT110 CT scanner, enabling qualitative comparison of resolution.

Table 10. Images of the density and spatial resolution tests from the XTE – CT test piece taken using a Medical CT scanner and the RTT110 CT scanner.

	Density in air test	Density in Perspex	Spatial resolution test
Medical CT	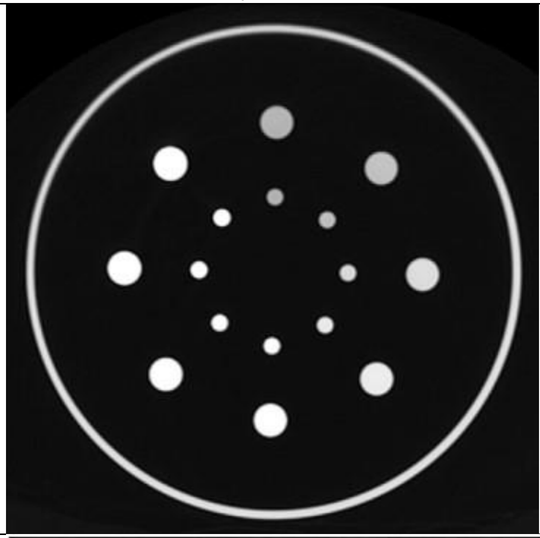	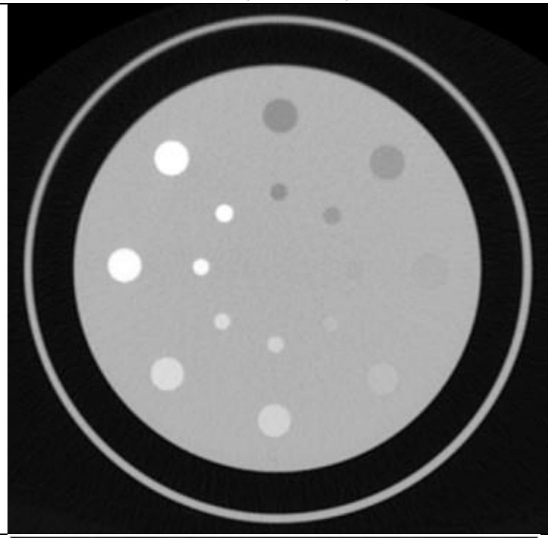	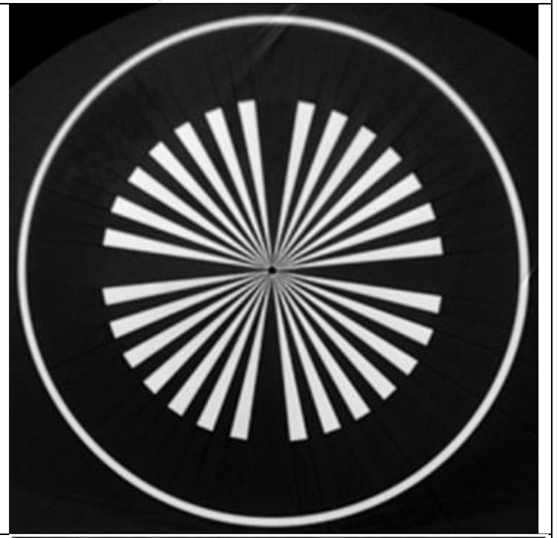
RTT110 CT	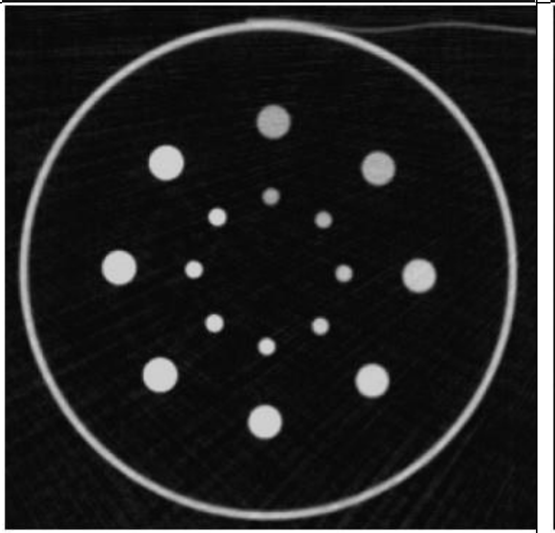	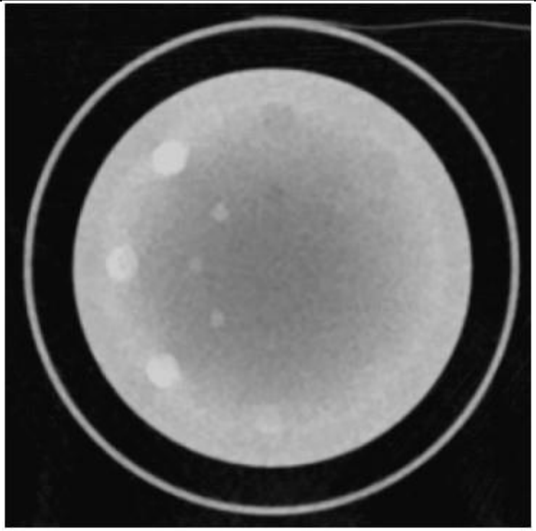	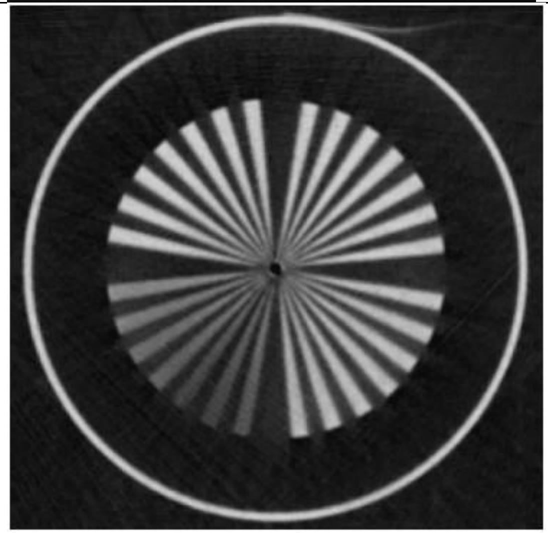

Table 11. Hu value comparison of materials within the 5 scans of the XTE-CT test piece. A region of interest containing 156 pixels was used for each measurement. Values are the mean, minimum, maximum and standard deviation of those 5 measurements. The "STDEV of pixels" is the standard deviation of the 156 pixels, with the value representing the mean of these 5 standard deviation values.

		Medical CT					RTT100 CT				
Material		Mean	Minimum	Maximum	Standard deviation	STDEV of pixels	Mean	Minimum	Maximum	Standard deviation	STDEV of pixels
Polypropylene	In Air	-135	-142	-120	8.71	7.42	-234	-247	-211	13.49	30.90
ABS	In Air	-60	-70	-53	7.00	6.66	-176	-193	-153	14.77	31.71
Polycarbonate	In Air	75	63	87	10.41	6.30	-59	-73	-35	14.13	30.74
Peek	In Air	156	144	166	7.94	5.95	10	-9	33	17.32	28.92
Delrin	In Air	305	297	316	7.58	6.34	146	129	179	19.48	30.33
PVC	In Air	366	354	375	10.68	7.04	549	528	582	20.23	45.15
PVDF	In Air	613	587	643	26.43	12.36	376	361	394	14.02	49.34
Teflon	In Air	928	891	977	44.36	20.66	632	603	664	23.59	40.45
Polypropylene	In Perspex	-94	-100	-81	7.94	12.95	-58	-76	-43	12.20	24.81
ABS	In Perspex	-28	-39	-15	8.40	11.44	-46	-58	-38	9.69	25.12
Polycarbonate	In Perspex	97	83	110	9.76	10.82	2	-24	21	18.45	29.86
Peek	In Perspex	176	161	184	9.76	9.86	28	6	47	14.46	31.87
Delrin	In Perspex	307	300	313	5.13	11.53	81	61	94	14.85	36.09
PVC	In Perspex	367	360	374	4.84	11.82	220	196	234	15.65	46.74
PVDF	In Perspex	597	573	619	17.98	14.33	202	180	226	17.61	46.91
Teflon	In Perspex	891	848	947	37.15	16.05	317	302	331	11.82	54.25

Table 12. Comparison of test values for the Medical CT and the Rapiscan RTT110. Tests include spatial resolution, 200mm dimension, and 40mm thickness. Values shown are the mean, minimum, maximum, and standard deviation of test values captured across 5 separate scans of the XTE-CT test piece.

	Mean	Minimum	Maximum	Standard deviation
	Spatial resolution test (mm)			
Medical CT	1.00	0.92	1.11	0.07
RTT110 CT	1.54	1.50	1.63	0.05
	Simple 200mm dimension test (mm)			
Medical CT	201	200	202	0.64
RTT110 CT	169	169	170	0.48
	Thickness test (resolution limited to count of 1mm slice widths)			
Medical CT	41	41	41	0
RTT110 CT	39	39	39	0

5. Discussion

This study demonstrates that the Rapiscan RTT-110 has good capacity to differentiate bone from soft tissue in beef primals and lamb carcases. On this basis we expect that the RTT-110 will provide imagery entirely suitable for identifying 3-dimensional skeletal landmarks for automation.

Bone tissue was consistently well differentiated from soft tissues in beef primals, however the RTT-110 prediction of CT bone % was substantially more precise in short loins than in rib sets. The reason for the reduced capacity of Rapiscan images to identify bone in rib sets is unclear, though may relate to the greater proportion of marrow in rib bones that is not differentiated from soft tissues. This is supported by Rapiscan images underestimating CT bone % by an average of 2.57 bone % units (± 0.49) in short loins compared to 3.21 % units (± 1.33) in rib sets. In lamb, RTT-110 scans consistently predicted CT bone % with high precision in all sections of the carcase.

The capacity of the Rapiscan RTT-110 system to differentiate fat and lean tissue in lamb or beef needs further development. While the approximate location of fat, lean and muscle seams could be visually identified upon qualitative assessment of RTT-110 images, determining fat and lean composition from RTT-110 scans via pixel value thresholding of fat and lean tissue produced highly variable results. While the RTT-110 scans of beef shortloins and lamb carcases predicted CT lean and fat % with good precision, this apparent ability of the RTT-110 to identify lean and fat tissue in these sections appears to be principally be a result of tissue thresholding in RTT-110 images incorrectly identifying the outermost tissues of primals (those with minimal tissue depth) as fat tissue. In beef short loins and lamb sections the majority of fat was located externally, resulting in the good precision of Rapiscan predictions of CT fat and lean composition. However, visual assessment of fat and lean tissue thresholding in RTT-110 images shown in Tables 5, 7, 8 and 9 demonstrates that tissue depth has primarily driven the identification of fat tissue in these images, with comparison to medical CT fat tissue identification demonstrating the error in Rapiscan fat identification. The incorrect identification of fat and lean tissue in RTT-110 images is particularly evident in beef rib set scans, where fat was incorrectly identified on the outermost edges of the primals (Table 5). The RTT-110 images failed to differentiate the fat tissue in these primals that is predominantly located internally between muscle groups, resulting in the poor precision of Rapiscan RTT-110 prediction of medical CT fat and lean % in beef rib sets.

With respect to dimension measurement, the RTT-110 demonstrated highly consistent 3-dimensional measurements across all sections of the scanned image. This was highlighted by both the precision (repeatability) of the 200mm dimension measurement, and the accuracy and precision of the thickness measurement. While the RTT-110 did show inaccuracy in its estimation of the 200mm measurement, reporting it as 169mm, this would be a simple matter of re-scaling these images to fix this inaccuracy. Furthermore, the resolution of the RTT-110 images was 1.5mm, comparing well with the medical CT scanner that had a resolution of 1mm. This resolution, and the capacity to estimate dimensions in a highly repeatable fashion demonstrate that the RTT110 would deliver image quality entirely adequate for automation. If additional resolution were required, then edge detection analysis would likely further enhance the existing image. Alternatively, while the RTT-110 was able to successfully differentiate materials of differing density, the voxel values showed markedly more variability than the corresponding voxel values from the medical CT scanner. This would align with the limited capacity of the RTT-110 to differentiate fat from lean, tissues with density values that only differ to a small extent, lean having an average density of 1.078g/cm^3, and fat 0.94 g/cm^3.

Therefore, further work is needed to calibrate RTT-110 images of beef primals and lamb carcasses to ensure that pixel values across the image are consistently associated with tissue density and not influenced by tissue depth. This would improve the ability to consistently differentiate fat and lean tissue between and within beef primals and lamb carcase sections, improving the estimation of carcass composition and allowing the accurate identification of seams between soft-tissue depots for the development of automation. Alternatively, the image resolution and capacity to measure in a highly repeatable fashion demonstrates the capacity of this device to provide imagery suitable for automation.

6. References

Gundersen, H., Bendtsen, T., Korbo, L., Marcussen, N., Møller, A., Nielsen, K., Nyengaard, J., Pakkenberg, B., Sørensen, F. & Vesterby, A. 1988. Some new, simple and efficient stereological methods and their use in pathological research and diagnosis. Apmis, 96, 379-394.

Gundersen, H. J. G. & Jensen, E. 1987. The efficiency of systematic sampling in stereology and its prediction. Journal of microscopy, 147, 229-263.

Mull, R. T. 1984. Mass estimates by computed tomography: Physical density from CT numbers. American Journal of Roentgenology, 143, 1101-1104.

Williams, A., Anderson, F., Siddell, J., Pethick, D., Hocking, E. J. & Gardner, G. 2017. Predicting lamb carcase composition from carcase weight and GR tissue depth. 63rd International Congress of Meat Science and Technology. Cork, Ireland, 729-732.